THE STUDY OF A CRYSTAL STRUCTURE BY X-RAY DIFFRACTION AND SOME MOLECULAR STRUCTURES BY ELECTRON DIFFRACTION

Thesis by

Chi-hsiang Wong

In Partial Fulfillment of the Requirements

For the Degree of

Doctor of Philosophy

California Institute of Technology

Pasadena, California

1957

ACKNOWLEDGMENT

I wish to express my appreciation to Professor Verner Schomaker, for without his patient guidance, acute criticism and warm friendship, this thesis would never have been written.

Thanks also to Dr. Richard Marsh for his generous help and constant encouragement on the crystal structure investigation.

To Mr. Alan Berndt for his stimulating collaboration on the investigation of the two polycyclohydrocarbons.

To Professors Saul Winstein and John D. Roberts and Drs. Edgar Smutny, Louis De Vries and George Guthrie, Jr. for supplying samples of several compounds for structural study.

To Professor Leo Brewer for advice on the properties of the cuprous chloride vapor.

To the California Institute of Technology, the Office of Naval Research, the Phi Beta Kappa Alumni and E. I. du Pont de Nemours and Co. (Inc.) for financial assistance.

ABSTRACT

The crystal structure of phenylcyclobutenedione has been investigated by the x-ray diffraction method. Three-dimensional techniques were used to deduce and to refine the trial structure. The space group is $P2_1/c$ with four molecules per unit cell.

Electron diffraction photographs have been made of cuprous chloride vapor. A six-membered alternating ring model of the trimer molecule with $\angle Cu\text{-}Cl\text{-}Cu \sim 90^\circ$ and very large amplitude of symmetric bending vibration seems plausible and is shown to be in agreement with the diffraction pattern.

The electron diffraction study of two light-heavy compounds ($Pb(CH_3)_4$, CF_3I) has verified the complex nature of the atomic scattering factors for electron diffraction. The bond lengths and bond angles of these two compounds are also determined.

The proposed structural formula of the polycyclohydrocarbon $C_{12}H_{14}$ (the 'cage') is consistent with the electron diffraction pattern. The average bond length was found to be longer than the normal C-C single bond length in both 'cage' and norbornane. A simple treatment based on a Hooke's law potential for bond stretchings and cross-ring repulsions gives pleasing agreement with the experimental result for the average bond lengths.

TABLE OF CONTENTS

I. The Crystal Structure of Phenylcyclobutenedione

Fig. 1 Phenylcyclobutenedione

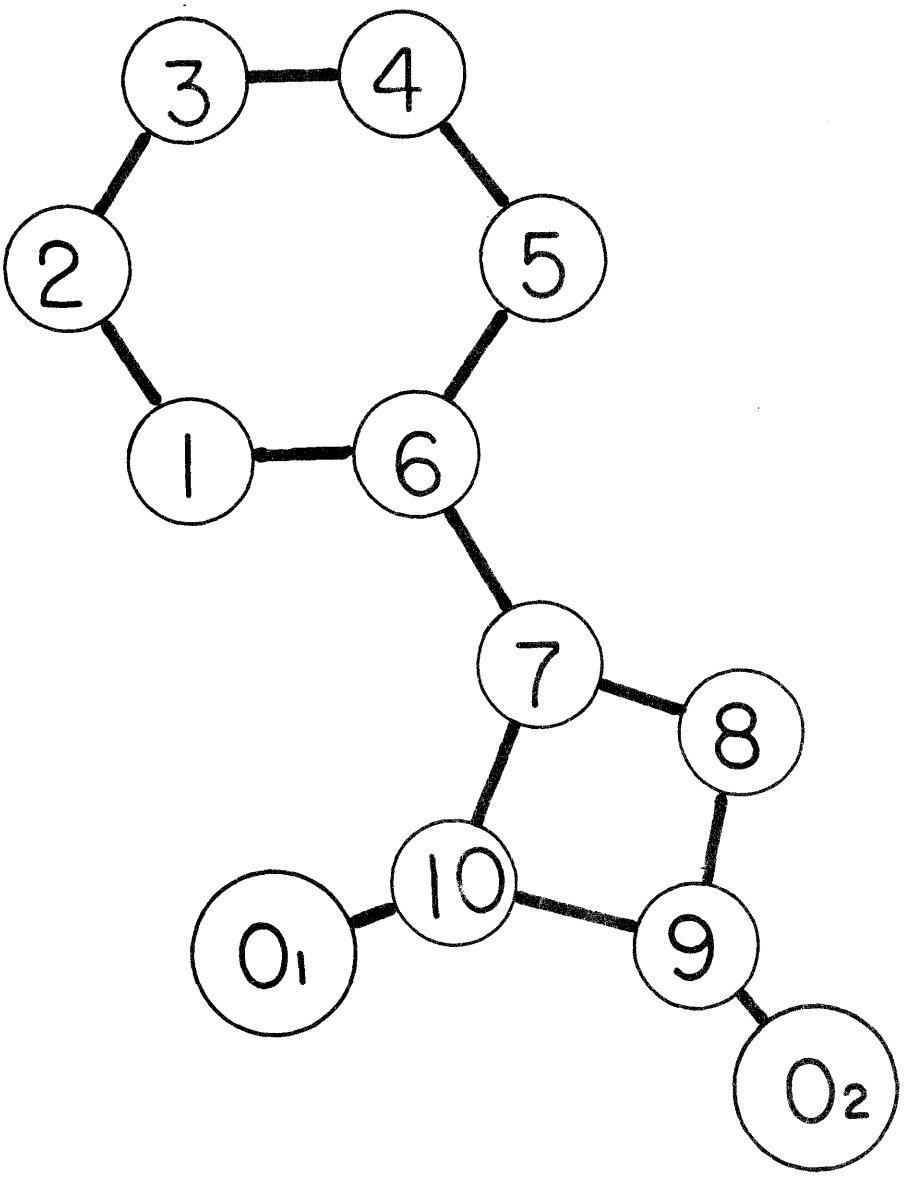

Phenylcyclobutenedione (PCBD), (fig. 1), was synthesized by Smutny and Roberts (1) in these Laboratories in 1952; it is apparently the first non-fused-ring derivative of cyclobutadiene ever prepared. Although the PCBD molecule would be expected to have about the same degree of ring strain as cyclobutadiene, PCBD, unlike cyclobutadiene*, is very stable up to about 150°. A precise crystal structure determination of PCBD would yield valuable information concerning bond lengths and bond angles in this interesting molecule, and might lead to an understanding of the cause of its stability. Knowledge of the bond lengths and bond angles in PCBD should also be valuable in furthering the general understanding of small ring compounds, many of which have been quite extensively studied in these Laboratories.

PCBD crystallizes from acetone solution in the form of yellow monoclinic needles. The needle axis is parallel to the crystal axis a. Rotation and multi-film equi-inclination Weissenberg photographs were prepared for the 0th through 6th layers around a, and 0th through 8th layers around b. For the a-axis photographs, needle-shaped crystals about 0.2 mm in diameter were selected; for photographs about the b axis, it was necessary to cleave the crystal and to shape it into cylindrical form with acetone-soaked filter paper, the resulting specimen again being about 0.2 mm in diameter. No correction for absorption was then deemed necessary.

---

* Molecular orbital calculation for cyclobutadiene (2), (3) predicts that it is very unstable, and organic chemists have been unsuccessful in their attempts to synthesize it.

The unit-cell constants a_o, c_o, and β were determined from a Straumanis-type* b-axis rotation photograph taken with Cr Kα radiation (λ = 2.2896 A). For this purpose, three high-angle reflections ($\underline{6}\ \underline{0}\ \underline{\bar{4}}$, $\underline{6}\ \underline{0}\ \underline{\bar{2}}$, and $\underline{3}\ \underline{0}\ \underline{\bar{10}}$) were used for which the sin θ values are 0.9928, 0.9824, and 0.9706. Subsequently, the spacings of a number of other $\underline{h}\ \underline{0}\ \underline{\ell}$ reflections were calculated from the determined cell constants; the results are in good agreement with the observed values (see Table 1). The value of b_o was determined from an $\underline{0}\ \underline{k}\ \underline{\ell}$ Weissenberg photograph for which the effective camera distance was deduced from the value of c_o and β previously obtained from the Straumanis photograph. The cell constants and estimated limits of error are:

$$a_o = 7.000 \pm 0.005 \text{ A}$$
$$b_o = 9.287 \pm 0.020 \text{ A}$$
$$c_o = 12.340 \pm 0.005 \text{ A}$$
$$\beta = 103.31 \pm 0.3^\circ$$

---

* The Straumanis method has the advantage that the effective camera distance may be precisely determined, thus eliminating radius and film shrinkage errors from the cell constants determination.

Table 1. List of sin θ for observed and calculated $\underline{h}\ \underline{0}\ \underline{\ell}$ reflections.

Reflections	$(\sin\theta_{Cr})_{obs}$	$(\sin\theta)_{calc}$
$(\underline{6}\ \underline{0}\ \underline{\bar{4}})$	0.9928	0.9928
$(\underline{6}\ \underline{0}\ \underline{\bar{2}})$	0.9824	0.9824
$(\underline{3}\ \underline{0}\ \underline{\bar{10}})$	0.9706	0.9706
$\underline{4}\ \underline{0}\ \underline{4}$	0.8442	0.8457
$\underline{4}\ \underline{0}\ \underline{\bar{2}}$	0.6548	0.6553
$\underline{2}\ \underline{0}\ \underline{\bar{2}}$	0.3467	0.3462
$\underline{2}\ \underline{0}\ \underline{0}$	0.3350	0.3365

The absence of reflections $\underline{0}\ \underline{k}\ \underline{0}$ with $\underline{k}$ odd and $\underline{h}\ \underline{0}\ \underline{\ell}$ with ℓ odd indicates the presence of a screw axis parallel to $\underline{b}$ and a glide plane perpendicular to $\underline{b}$ with a glide component of $c_o/2$; thus, the probable space group is $P2_1/c$. The density determined by the flotation method, 1.42 gm/cc, agrees with the value 1.44 gm/cc calculated on the basis of four PCBD molecules per unit cell.

Complete three-dimensional intensity data out to sin θ = 0.956 were collected* using copper radiation and the multi-film equi-inclination

---

* $\underline{2}\ \underline{2}\ \underline{\ell}$ on the a-axis photograph and $\underline{h}\ \underline{2}\ \underline{\ell}$ on the b-axis photograph were not estimated because of contamination by iron radiation reflections from other layers.

Weissenberg technique. Within this limiting sphere about 1470 independent reflections are permitted by the space group. Of these about 400 were too weak to be observed. The intensities were estimated visually with the aid of an intensity strip prepared from the same crystal. The intensities of the stronger reflections were estimated on two or even three films from the same multi-film exposures. The film factor was assumed to be $\exp(k\sec\nu)$ where ν is the inclination angle. The constant k was evaluated from the zero-layer film factor determined by comparing a few carefully selected zero-layer reflections. This form of film factor is designed to account for the increase of effective thickness of the film as a function of the inclination angle. For those reflections whose intensities were estimated from more than one film, weighted averages were taken, with lower weight for very strong and very weak readings. Corrections for Lorentz and polarization factors were carried out on IBM machines giving a set of related F^2 values for each layer line about the a and b axes.

The correlation factors for putting these F^2 values from different layer photographs onto the same scale were determined by the following method: The ratios

$$R_{ij} = (F^2_{h_i k_j \ell})_a / (F^2_{h_i k_j \ell})_b$$

obtained from the ith layer of the a-axis photographs and the jth layer of b-axis photographs were averaged for all ℓ's, (again, with the exception of very strong and very weak readings). From the resulting sets of

averaged ratios, the interlayer correlating factors G_{mn} were evaluated as

$$G_{mn} = \left(\sum_j R_{mj} w_{mj} \Big/ \sum_j w_{mj}\right) \Big/ \left(\sum_\ell R_{n\ell} w_{n\ell} \Big/ \sum w_{n\ell}\right)$$

where W_{mj} is a weighting factor roughly proportional to the inverse of the average deviation of R_{mj}. Then the final set of interlayer correlation factors G'_{mn} were evaluated as

$$G'_{mn} = \left(\sum_{j=0}^{L} G_{mj} G_{jn}\right) \Big/ L$$

With these correlation factors, all the corrected intensities were put on the same arbitrary scale; for those which had been measured on both a and b axes photographs, averages were taken. To check the accuracy of the visual data, F_a^2 and F_b^2 were compared; the two sets of values usually agreed within 20%.

The next step was to establish the absolute scale of the observed F's and to evaluate the average isotropic temperature factor; this was done by Wilson's statistical method (4). Wilson's method is based on the hypothesis that in a spherical shell of approximately constant $\sin^2\theta$ the average value of F^2 is equal to

$$\sum_i f_i^2 \exp(-2B \sin^2\theta/\lambda^2)^*$$

where the sum is taken over all the i atoms in the unit cell. A plot of $\ln(\Sigma F_o^2/\Sigma\Sigma_i f_i^2)$ versus $\sin^2\theta$ is given in figure 2. The slope of the straight line is equal to twice the temperature factor; thus $(+2B) = 3.3(\lambda^2 c_u)$. The intercept, $\ln(\Sigma F_o^2/\Sigma\Sigma_i f_i^2) = -1.7$, is the log of the scale factor - the factor necessary to reduce the observed F^2 value to an absolute scale.

With the corrected F^2 values and the average temperature factor, the three-dimensional Patterson function

$$P(u\,v\,w) = \frac{4}{V_o}\sum_{hkl} A_H \cos 2\pi(\underline{H}\cdot\underline{U})$$

was calculated; here V_o is the volume of the unit cell, $\underline{H}$ is the reciprocal lattice vector ($h\underline{a}^*$, $k\underline{b}^*$, $l\underline{c}^*$) and $\underline{U}$ the Patterson space vector ($\underline{u}$, $\underline{v}$, $\underline{w}$). The coefficients were taken as

$$A = \left\{ \frac{F_o^2(h\,k\,l)}{\sum_i f_i^2 \exp(-2B\sin^2\theta/\lambda)} - 1 \right\} M(\sin\theta)$$

in order to remove the peak in the origin and to sharpen the other peaks for gaining better resolution. The function

$$M(\sin\theta) = \frac{4\pi^2}{f_H\lambda^2}\sin^2\theta \exp\left(-\frac{4\pi^2}{p^2\lambda^2}\sin^2\theta\right) ,$$

---

* McWeeny's form factors were used throughout this investigation.

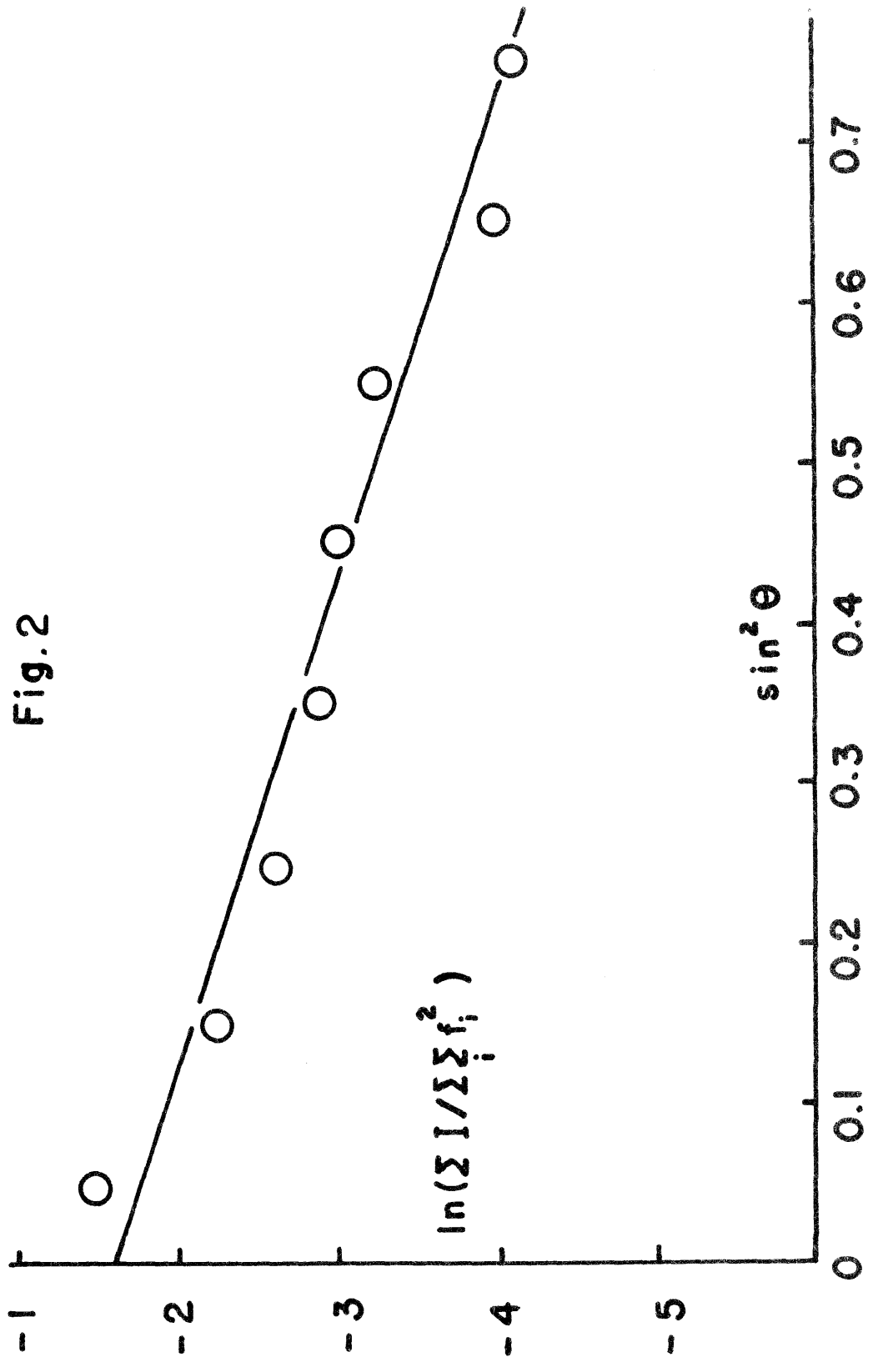
-1
-2
-3
-4
-5
$\ln(\Sigma I/\Sigma\Sigma f_i^2)$
0
0.1
0.2
0.3
0.4
0.5
0.6
0.7
$\sin^2\theta$

Fig. 2

where $p = 4.5$, is the modification function designed for the latter purpose. The ranges of computation were: a, 0 - 15/30; b, 0 - 30/60; and c, 0 - 60/60. The corresponding intervals are 0.22, 0.15 and 0.20A.

The Patterson showed that practically all the interaction peaks lie on two planes oriented approximately parallel to $(20\bar{1})$ and separated by a distance $a_o/4$ (the $(20\bar{1})$ plane is nearly perpendicular to the a-axis). Thus, just from the general distribution of the Patterson peaks, it was apparent that the PCBD molecule is approximately planar and that it lies roughly in the $(20\bar{1})$ plane; furthermore, it appeared that the long molecular axis must lie about 30° inclined from the b-axis. However, without a careful analysis of the complete Patterson function, the actual position of the molecule in the cell is not defined. With the help of some low order h 0 ℓ structure factor maps, the approximate position of the molecule projected on the (010) plane was found. Appropriate x and z parameters were evaluated based on the molecular configuration shown in fig. 1 and on normal bond lengths and bond angles. The position of O_1 could not be determined; i.e., O_1 might have been attached to C_8 or to C_{10}. A complete set of h 0 ℓ structure factors was then calculated, assuming that O_1 was attached to C_{10}; the resulting reliability factor $R = \sum |F_o - F_c| / \sum |F_o|$ was 0.38, a reasonable value for a centrosymmetric crystal. An h 0 ℓ Fourier synthesis was computed using the signs obtained from the structure factor calculations. The result of this Fourier synthesis (fig. 3) not only confirmed the position of O_1 (i.e., O_1 is attached to C_{10}), but also indicated the degree of tilt (about 13°) of the molecular plane from $(20\bar{1})$. A second set of structure factors

Fig. 3 hOl Fourier

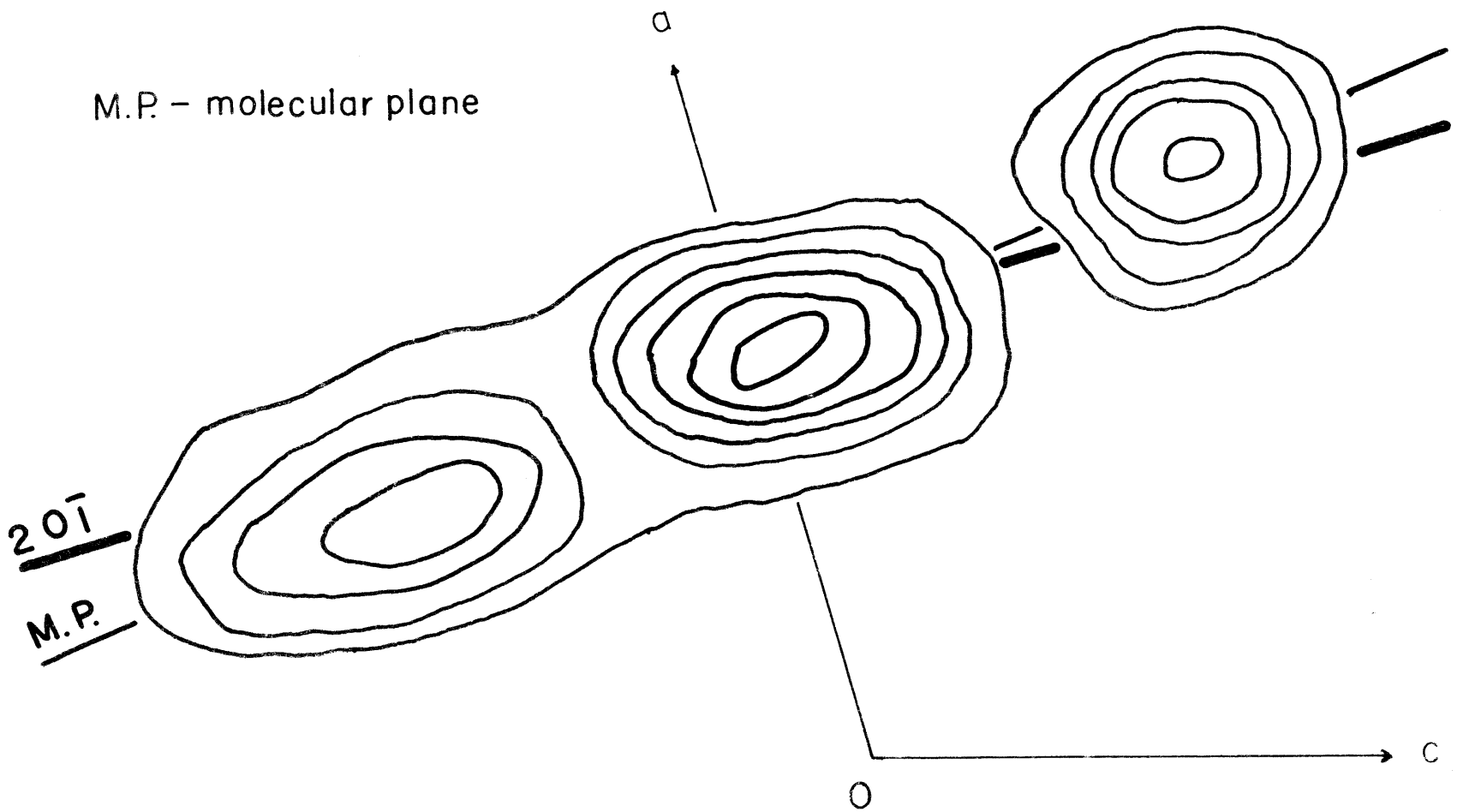

O
O2
8
9
7
10
O
1
2

was calculated but because of the severe overlap on the $h\ 0\ \ell$ projection the parameters were not further refined. At this stage the R factor for the 71 $h\ 0\ \ell$ reflections was 0.29.

In order to investigate the y parameters, three sets of $0\ k\ \ell$ structure factors were calculated, using the z parameters based on the previous $h\ 0\ \ell$ Fourier and y parameters deduced from three trial structures whose positions relative to the b and c axes are shown in fig. 4. These three structures were deduced from a few low order $0\ k\ \ell$ structure factor maps. This time, due to the hypersymmetry of the molecule, the structure factor map failed to finger out a unique structure, and results of the structure factor calculation were rather disappointing. However, as a consolation, there were about ten low order reflections (apart from $0\ 0\ \ell$) in the (B) case showing some promise for structure 'B'. An $0\ k\ \ell$ Fourier containing about 30 selected reflections with signs obtained from structure 'B' was calculated, and the result was a complete failure in that no sensible conclusion could be drawn.

Struggling against frustration, we decided that to go back and solve the Patterson function methodically and systematically was the best way out. First, for the convenience of interpretation, the Patterson function was replotted on sections parallel to $(20\bar{1})$ (previously it had been plotted on sections parallel to (010)). Then, with the assumption of a planar molecule oriented parallel to $(20\bar{1})$ (this assumption was purely for simplicity's sake, since, as previously stated, the molecule is tilted about 13° out of the $(20\bar{1})$ plane), the problem is reduced essentially to a two-dimensional one; the atomic parameters in this plane are y and $(z - x/2)$. The Patterson function, in the present case, is

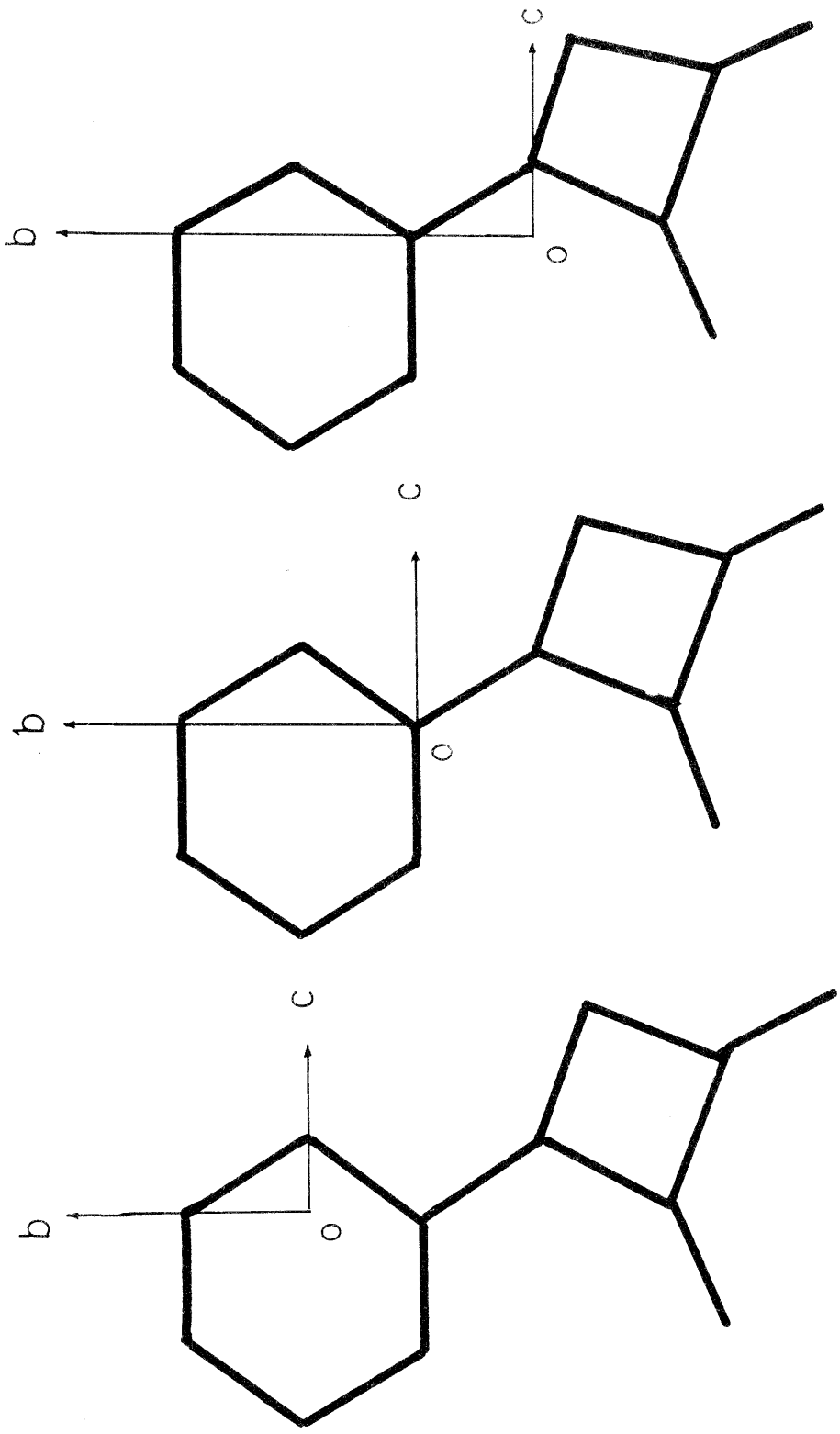

Fig.4

separated into four unmixed sets of vectors: (A) vectors due to the intramolecular interactions; (B) vectors due to interactions between molecules related by the 2_1 axis; (C) vectors due to the interactions between molecules related by the glide plane; and, finally (D) vectors due to interactions related by the center of symmetry. Thus we might proceed to solve these four sets independently. The solution of (A) would give the molecular structure; the solution of (B), the orientation of the molecule about the 2_1 axis; the solution of (C), the orientation about the glide plane; and the solution of (D), the orientation about the center, which would provide a check for the values obtained from (B) and (C). However, in the present case, the parameters could not be evaluated uniquely and accurately for the following reasons. First, because of the hypersymmetry of the molecule, more than one apparently satisfactory way of packing of the molecule in the unit cell could be fitted with the Patterson function. (Thus, vector sets (B), (C) and (D) could be interpreted in more than one way.) Secondly, because of the use of the modification function for sharpening the interaction peaks, the relative weight of each interaction was perturbed by the ripples generated from the neighboring peaks, and hence a precise determination of the parameters was not considered as feasible.

At any rate, four possible ways of packing were found from the Patterson; two of them were immediately ruled out by undesirable packing distances and by the previously calculated $\underline{h}\ 0\ \underline{\ell}$ Fourier. The remaining two differed only in the $\underline{y}$ parameters of the atoms. One set of $\underline{y}$ parameters was approximately 0.1 A from those derived from model (B),

and the other set was about half way between (B) and (C). For both cases the newly obtained ($\underline{x} - \underline{z}/2$) parameters were in good agreement with those obtained from the $\underline{h}\ \underline{0}\ \underline{\ell}$ data. $\underline{0}\ \underline{k}\ \underline{\ell}$ structure factors calculated for these two models gave R factors of 0.59 and 0.46 respectively. The former, like model B, had better agreement for low order reflections, and was tentatively accepted as the 'right' structure.

Structure factors for two layers, $\underline{0}\ \underline{k}\ \underline{\ell}$ and $\underline{1}\ \underline{k}\ \underline{\ell}$, were calculated from the parameters of the 'right' structure, and about 100 selected reflections were included in a three-dimensional least squares calculation; only the diagonal terms of the matrix of the normal equations were calculated, and unit weight was assigned to each of the reflections. Many of the indicated parameter shifts were as large as 0.15 A. Structure factors of about 300 reflections within the sphere $\sin\theta \leq 0.46$ were calculated from the new set of parameters. Subsequently, two more least squares were calculated using all 300 reflections ($\sin\theta \leq 0.46$) with the exception of those of doubtful signs, and the R factor was reduced to 0.39. At this point, some of the bond lengths deduced from the new set of parameters became unreasonable, and a three-dimensional Fourier synthesis seemed to be in order. The three-dimensional Fourier series

$$\rho(\underline{x}\ \underline{y}\ \underline{z}) = \frac{4}{V_0}\sum_{hk\ell} F \cos 2\pi\,(\underline{H}\cdot\underline{X})$$

was calculated with low order reflections ($\sin\theta \leq 0.46$) within the range $\underline{x}$ from 0 to 30/30, $\underline{y}$ from 0 to 15/30, and $\underline{z}$ from 15/60 to 45/60, where $\underline{X}$

is ($\underline{x}$, $\underline{y}$, $\underline{z}$), the general vector in real space. A slice of the resulting electron density plot through the molecular plane is reproduced in fig. 5; it clearly shows a reasonable position and weight for every heavy atom. At this point all doubt concerning the correctness of this structure evaporated, and it appeared that the remaining work would be further refinement of the parameters.

Because no high order reflections were involved in the three-dimensional Fourier synthesis, the resulting peaks in the electron density map appeared to be rather flat; hence only an unexact (but improved) set of positional parameters was deduced. A new set of structure factors was calculated from the improved parameters including all reflections for $\sin \theta \leq 0.64$ (about 500 in number); the resulting R factor was 0.36. One more least square treatment reduced R to 0.21.

Structure factors were then calculated for all the recorded data (1213 reflections); the R factor was 0.23. Two more least squares did not alter the R factor, although some of the parameter shifts were as large as 0.05 A. At this stage, the necessity of making a difference Fourier synthesis was realized.

It was hoped that a difference Fourier might reveal a number of valuable pieces of information concerning the crystal structure, such as the shifts of the atomic positions, the positions of the hydrogen atoms, and the anisotropic temperature factor effects.

Accordingly, a three-dimensional difference Fourier synthesis

$$D = \frac{4}{V_o} \sum_{hkl} (F_o - F_c) \cos 2\pi (\underline{H} \cdot \underline{X})$$

Fig. 5

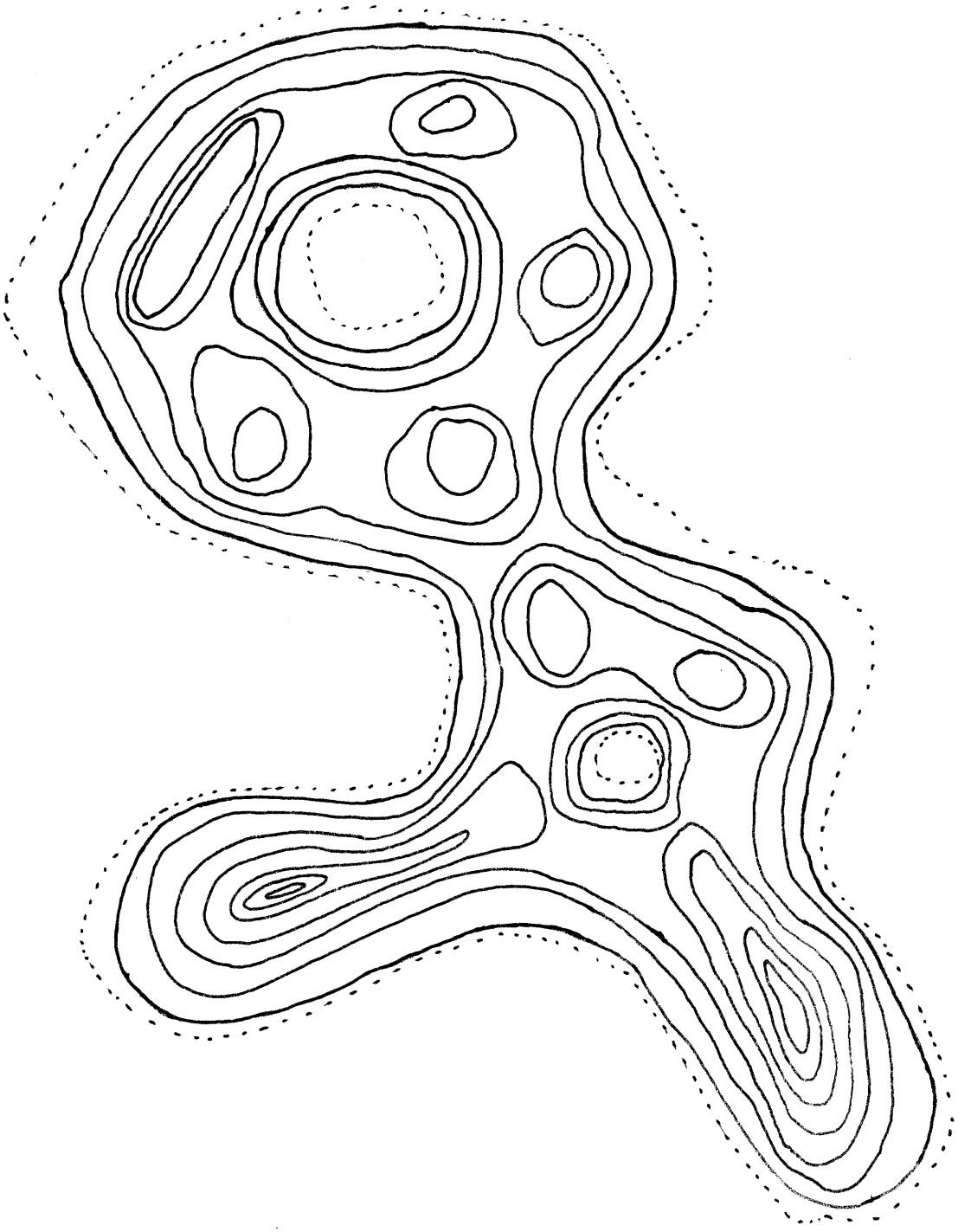

was calculated (with the complete data), with the same intervals and ranges as those for the calculation of the three-dimensional Fourier synthesis.

In the difference map, positive regions appeared at or near the positions expected for all the hydrogen atoms except the one bonded to C_4; however, many of the peaks were badly distorted. The general appearance of the difference map might be naively described in terms of the molecule undergoing a seesaw motion in the crystal with the pivotal point located on the C_6-C_7 bond. The indicated motion is practically normal to the molecular plane. In addition, the benzene ring itself appears to have an in-plane rocking motion. The two carbonyl oxygen atoms exhibit much greater out-of-plane motion than their bonded carbon atoms. Of course, the indicated anisotropy is a combined effect due to the actual anisotropic thermal motion of the atoms in the crystal previously assumed to be isotropic, and to the discrepancies between the assumed spherical distribution of electrons and the actual distribution of electrons of a bonded atom. The anisotropic temperature factor correction was evaluated by a method due to Cochran (5), who assumes that the electron distribution of an atom under anisotropic thermal vibration may be considered to be ellipsoidal in shape. Then the temperature factor of such an atom is

$$T = \exp\left(-\sum_i \beta_i h_i^2\right)$$

where

$$q_i = B + \Delta B_i$$

are the thermal vibration parameters in directions i, (i = 1,2,3, for the three principal axes of the ellipsoid of vibration), and h_i is the component of $\sin\theta/\lambda$ in the direction i. The correction ΔB_{ij} evaluated from the difference map for a centrosymmetric orthogonal cell is

$$\Delta B_{ij} = \frac{3V_0\lambda^4}{64\pi^2 \sum_{hkl} f_j \sin^4\theta} \left\{ 4\frac{\partial^2 D}{\partial r_{ij}^2} - \frac{\partial^2 D}{\partial r_{2j}^2} - \frac{\partial^2 D}{\partial r_{3j}^2} \right\} \cdot \frac{1}{8}$$

where r_{ij} is the principal axis i of the ellipsoidal atom j. The equivalent expression of T (6) is

$$T_1 = \exp\left\{ -\sum_i q_i \left(h g_{i1} a^* + k g_{i2} b^* + l g_{i3} c^* \right)^2 \right\}$$

for the two atoms related by the center where the g_{i1}, g_{i2} and g_{i3} are the direction cosines of the principal axis i with respect to a^*, b^* and c^*, and

$$T_2 = \exp\left\{ -\sum_i q_i \left(h g_{i1} a^* - k g_{i2} b^* + l g_{i3} c^* \right)^2 \right\}$$

for the other two equivalent atoms related to the above pair by a glide plane or a screw axis. Then, the structure factor for these atoms of $P_{2_1/c}$ space group is

$$F = 4\sum_n \left\{ \bar{f}_n \cos 2\pi(hx_n + lz_n) \cos 2\pi k y_n - \Delta f_n \sin 2\pi(hx_n + lz_n) \cdot \sin 2\pi k y_n \right\}$$

for $(k + l)$ even, and

$$F = 4\sum_n \left\{ -\bar{f}_n \sin 2\pi(hx_n + lz_n) \sin 2\pi k y_n + \Delta f_n \cos 2\pi(hx_n + lz_n) \cdot \cos 2\pi k y_n \right\}$$

for $(k + l)$ odd, where

$$\bar{f} = \frac{1}{2}(T_1 + T_2) f$$

and

$$\Delta f = \frac{1}{2}(T_1 - T_2) f$$

The shifts of the atomic positions were evaluated from an equation,

$$\Delta x_i = -\left(\frac{\partial D}{\partial x_i}\right) / C_i$$

where C_i is the curvature of atom i in the electron density map.

Because of the interaction between the hydrogen peaks and the anisotropy corrections around the benzene ring, neither the positions of the hydrogen atoms nor the anisotropic temperature factors of the benzene carbons could be evaluated accurately. Therefore, a new set of structure factors was calculated with the indicated temperature factor correction applied to the atoms of the cyclobutenedione group and with calculated hydrogen positions (assumed C-H 0.9 A) (7); the result showed some improvement. A second difference Fourier was then calculated. The new summation indicated excellent results for the previous correction on the cyclobutenedione group. The benzene ring appeared to be the same as in the previous difference map as expected; however, the absence of hydrogen peaks indeed made the interpretation much easier. The newly evaluated temperature factors for all the heavy atoms are listed in Table 2, and the parameter shifts and the new parameters, in Table 3. At this point, the structure determination is already reaching the final stage, although a few rounds of refinement are still needed to bring it to the desirable precision. As it stands now, the author believes that the maximum parameter shifts still can be as large as 0.03 A, and the average parameter shifts would be about 0.01 A in the next refinement, which will be carried out later on the new Datatron computer.

Table 2

The anisotropic corrections of the temperature factor

Atom	α^1 10^{-3}	β^1 10^{-3}	γ^1 10^{-3}	η^1 10^{-3}	δ^1 10^{-3}	ε^1 10^{-3}
1	1.3	-0.2	0	0	0	0
2	6.6	4.0	0.8	0.4	0	0
3	5.3	1.1	0.8	0.6	0	1.2
4	5.7	1.1	1.9	1.5	0	0
5	0	0	0	0	0	0
6	-0.6	-1.3	-0.8	-0.6	0	0
7	0.4	-3.2	-0.3	-0.2	0	0
8	2.3	-0.7	-0.5	-0.3	0	0
9	6.9	0.3	0	0	0	0
10	5.6	-0.8	-0.5	-0.4	0	0
O_1	6.2	3.3	-1.4	-1.0	0	0
O_2	10.9	1.2	0	0	0	0

1 $T = \exp\left(-B\frac{\sin^2\theta}{\lambda^2} - \sum_i \sigma B_i h_i^2\right)$

$= \exp -(0.023h^2 + 0.012k^2 + 0.007l^2 + 0.006hl)$

$-(\alpha h^2 + \beta k^2 + \gamma l^2 + \eta hl + \delta hk + \varepsilon kl)$

Table 3

Latest shifts and parameters obtained from the second difference map

Atom	Latest shifts			Latest parameters		
	$(\Delta x'/a)^*$	$(\Delta y'/b)^*$	$(\Delta z'/c)^*$	$(x'/a)^*$	$(y'/b)^*$	$(z'/c)^*$
1	.0000	.0000	.0021	.1780	.5356	.3731
2	.0056	.0000	.0047	.1389	.6645	.3177
3	.0022	.0000	.0035	.1670	.7929	.3765
4	.0000	-.0048	-.0016	.2370	.7882	.4918
5	.0000	-.0026	.0007	.2786	.6594	.5498
6	-.0069	-.0019	-.0022	.2447	.5311	.4867
7	.0000	.0000	-.0017	.2842	.3916	.5425
8	.0048	.0000	.0007	.3480	.3514	.6519
9	-.0014	-.0011	.0030	.3441	.1913	.6244
10	.0043	.0000	.0000	.2684	.2368	.4996
O_1	.0000	.0000	.0041	.2220	.1810	.4123
O_2	.0000	.0000	.0000	.3817	.0797	.6750

* $x' = ax$.

Discussion of the structure:

The PCBD molecule is planar as the present result indicates (see later discussion). These planar molecules are packed practically parallel to each other throughout the crystal as may be seen from the projection of the structure onto the (010) plane, shown in fig. 6. A drawing of the structure projected onto $(20\bar{1})$ is shown in fig. 7; in this drawing, all the significant intermolecular distances are indicated. Each molecule is embraced by twelve closest neighbors, and the contacts to all of those twelve neighbors are at the normal van der Waals distances. These twelve neighbors may be conveniently separated into four groups. Two of the neighbors are related to the reference molecule by a translation along b (group 1); two others, which sandwich the reference molecule in the a direction, are related to it by the centers of symmetry (group 2). The remaining eight neighbors are located at the eight corners of an orthorhombic block which contains the reference molecule; four of them are related to the reference molecule by the 2_1 axes (group 3), and the other four by the glide planes (group 4). Groups 3 and 4 may be identified in fig. 7.

In the crystal, the PCBD molecules are arranged in layers approximately parallel to $(20\bar{1})$, as is shown again in fig. 6. But these layers are not dense and this is not a typical layer structure with weak intermolecular bonding between layers and strong bonding within layers; instead, the van der Waals' contacts are distributed rather uniformly in all directions around each molecule (fig. 7). The absence of a preferred cleavage is therefore not surprising.

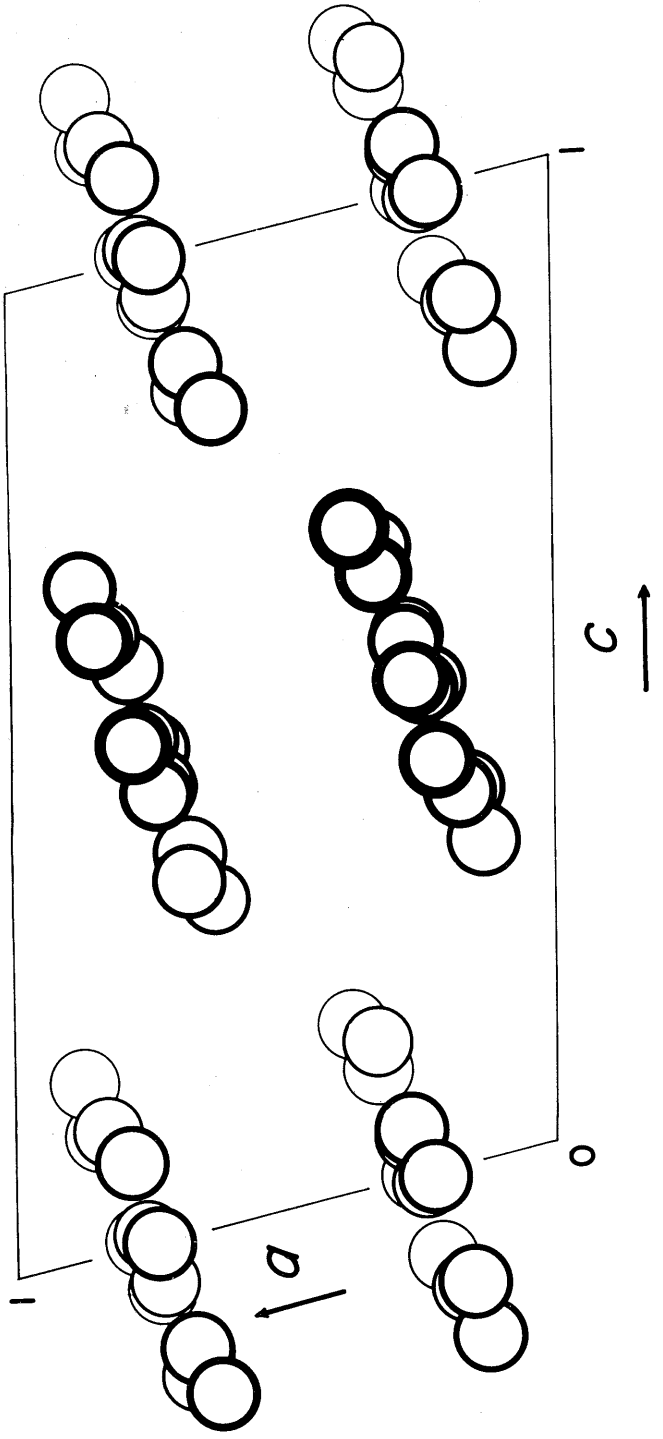

Fig. 6

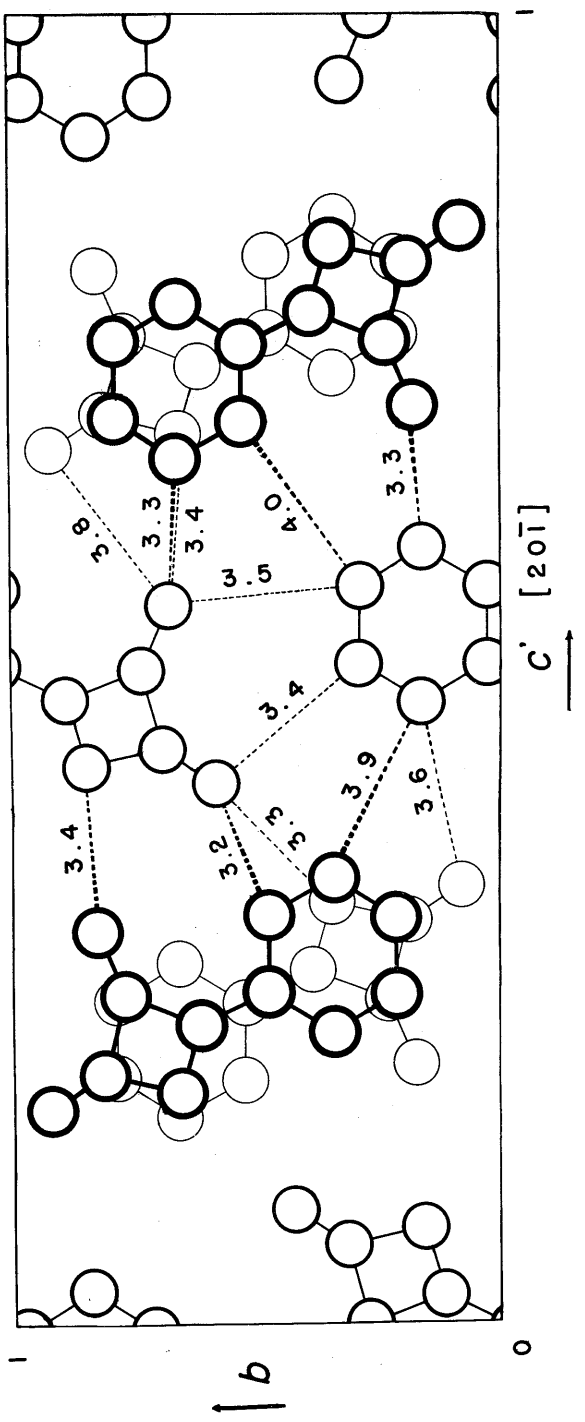

Fig. 7

The density (1.42 gm/cc) and melting point (119°-120°) (1) of the PCBD crystal are quite comparable with other quinone crystals, such as p-benzoquinone (1.32 gm/cc; 115.7°) (8) and α-naphthoquinone (1.422 gm/cc; 125°) (8). However, PCBD, which decomposes at 150° (1) is not as stable as the other quinones. This is probably due to the strain energy in the four-membered ring which is not present in the other above-mentioned quinones.

At the present stage of refinement, a detailed discussion of the molecular structure of the PCBD is probably not warranted. Nevertheless, a few remarks on some of the structural features might be made; i.e., features which can be compared to well-known examples, and features which can be considered to have well-established characteristics immune to future refinements.

From the list of positional parameters in Table 3, all the bond lengths and bond angles together with the best planes for the benzene ring and for the four-membered ring were evaluated. The bond lengths and bond angles are shown in fig. 8.

In the benzene ring, the average bond length, 1.39 A (range from 1.37 to 1.41 A), and the bond angles (range from 117° to 122°), are compatible with the usual values for a normal benzene ring. The normalized best plane for the benzene carbon atoms, deduced from a least-squares treatment, is

$$0.9933x' + 0.03289y' - 0.3388z' + 0.1650 = 0 .$$

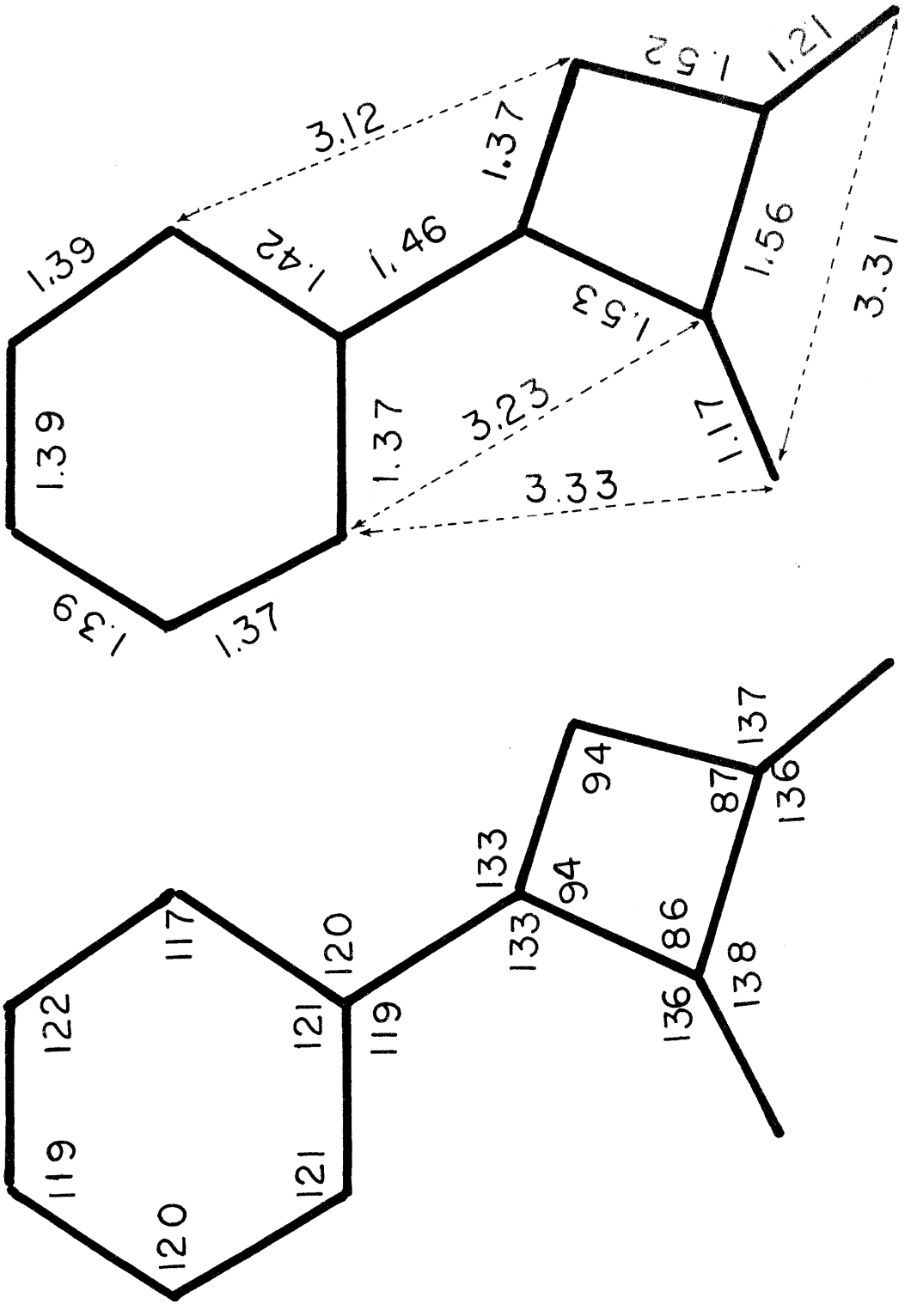
1.39
1.39
1.39
1.37
1.37
1.46
1.42
3.12
1.37
1.52
1.21
1.56
3.31
1.53
3.23
3.33
1.17
117
120
122
121
119
119
121
120
133
133
94
94
87
86
136
138
137
136

Fig. 8

The deviations of the benzene carbons from this plane are listed in Table 4; no deviation is greater than 0.01 A. In view of the uncertainty of the parameters corresponding to the incomplete refinement of the structure, the degree of coplanarity of the benzene ring may be fortuitous; on the other hand, this apparent coplanarity may be attributed to the hypersymmetry of the molecule which could cause the atomic parameters to remain "locked" in a coplanar arrangement during the early refinements.

The normalized best plane for the four-membered ring also deduced by least square is

$$0.9957x' + 0.0495y' - 0.3293z' + 0.0170 = 0$$

and the deviations for the four atoms from this plane, listed in Table 4, are also less than 0.01 A. Although the two carbonyl oxygen atoms were not included in the calculation of the best plane, they are indeed lying in the same plane (Table 4).

The calculated dihedral angle between these two planes is smaller than 1°. The deviations of the four-membered ring from the benzene plane are also reasonably small (Table 4). Thus, the conclusion is that the present result suggests that the PCBD molecule is planar.

The bridge between the two rings, the C_6-C_7 bond, appears to be considerably shorter than the normal single-bond distance of 1.54 A; the

Table 4

Deviations from the best plane of the benzene ring

Atom	Δ(A)
1	0.006
2	0.005
3	-0.006
4	-0.003
5	0.004
6	-0.006
(7)*	-0.008
(8)*	-0.033
(9)*	0.005
(10)*	0.015

Deviations from the best plane of the cyclobutene ring

7	0.003
8	-0.005
9	0.005
10	-0.003
$(O_1)^*$	-0.002
$(O_2)^*$	0.012

* not included in the calculations.

shortening may be attributed to resonance. This resonance is probably the main cause of the stability of the PCBD molecule. We shall defer any estimate of the importance of this resonance until the C_6-C_7 length has been more accurately measured.

The bond lengths and bond angles of the four-membered ring - very important items in this investigation - will not be discussed here, since small deviations are to be regarded as critical and meaningful, and the present parameters are not competent to indicate such deviations. However, it is clear that r_{78} is a double bond and the other three bond distances are all of the right order of magnitude for C-C single bonds. The average of the carbonyl C-O distance, 1.19 A is also comparable with the usual value, 1.21 - 1.23 A.

The result that the bond angles $\angle$1-6-7 and $\angle$5-6-7 are equal is expected, but the equality of $\angle$6-7-8 and $\angle$6-7-10 is very remarkable. In the case of isobutene (9) the corresponding angles are $\angle$6-7-10 $\sim 110^\circ$ and $\angle$6-7-8 = $\angle$8-7-10 $\sim 125^\circ$. In PCBD, however, $\angle$8-7-10 is compressed to 94° due to the formation of the four-membered ring; in order to compensate for the compression of $\angle$8-7-10, both $\angle$6-7-10 and $\angle$6-7-8 are stretched, and our result seems to suggest that $\angle$6-7-10 is stretched twice as much as $\angle$6-7-8. This result may, perhaps, be interpreted as due to the difference of bending force constants for the propane carbon skeleton (0.3×10^5 dyne/cm) (10) and the propene carbon skeleton (0.6×10^5 dyne/cm) (11) as reported by the infrared investigations. A different result, $\angle$6-7-8 being much greater than $\angle$6-7-10, reported in the investigation of 1-methyl cyclobutene (12), may well be in error.

References

1. E. J. Smutny and J. D. Roberts, J. Am. Chem. Soc., 77, 3420 (1955).
2. W. G. Penney, Proc. Roy. Soc. A, 146, 223-38 (1934).
3. C. A. Coulson and W. E. Moffitt, Phil. Mag., 40, 1-35 (1949).
4. A. J. C. Wilson, Acta Cryst., 2, 318-21 (1949).
5. W. Cochran, Acta Cryst. 4, 408-11 (1951).
6. J. S. Rollet and D. R. Davis, Acta Cryst., 8, 125-28 (1955).
7. R. E. Marsh, Private notes.
8. Handbook of Chemistry and Physics, 1950-1951.
9. J. P. McHugh, Private notes.
10. E. B. Wilson, Jr. and A. J. Wells, J. Chem. Phys., 9, 319-22 (1951).
11. D. M. Gates, J. Chem. Phys. 17, 393-8 (1949).
12. W. Shand, Jr., V. Schomaker and J. R. Fischer, J. Am. Chem. Soc., 66, 636-40 (1944).

II. An Electron Diffraction Investigation of the Structure of Cuprous Chloride Trimer

Cuprous chloride vapor was long regarded as dimeric, on the basis of early vapor density measurements, but in 1948 Brewer and Lofgren (1) reported it to consist of monomer and trimer with no dimer, and said that at 1000°K the saturated vapor should be 100.0 mole % trimeric. The present diffraction data are apparently similar to those obtained earlier by Maxwell and Mosley and not found to be entirely compatible with any dimer model (2); our interpretation in terms of the trimer differs, however, from Maxwell's. He reports (3) disagreement with "a six-membered ring structure" and agreement with "a configuration consisting of two sphenoids sharing an edge for the trimer in equilibrium with a relatively high concentration of the monomer." We find agreement with an alternating six-ring structure, of the sort proposed by Brewer and Lofgren ((1), p. 3044) to account for the stability and low entropy of the trimer as well as the relative instability of the dimer, but with a remarkably great amplitude of vibration toward and away from the configuration proposed (4) by Professor Pauling, in which "the copper atoms form a small triangle and the chlorine atoms a large triangle, each chlorine atom being bonded to two copper atoms and each copper atom being bonded to two chlorine atoms and also the two other copper atoms."

Experimental. Greenish cuprous chloride of C.P. grade was washed in dilute sulfuric acid to obtain a purified white powder which was heated to about 450°C in a simple monel-metal boiler inside our new electron diffraction camera. The photographs (Kodak-50 plates; $L \sim 10$ cm; $\lambda \sim 0.06$ A) were interpreted visually in the usual way (5).

The boiler had a total volume of 0.8 ml and was usually somewhat less than half full, so that the liquid sample surface was about 0.6 cm^2. The orifice was a tube about 1 mm long and 0.3 mm or 1 mm in diameter.

Results. Our photographs show about eight main rings (fig. 1), graced with a few weak, close-in outer shoulders (1, 3, a, and b); the radial distribution curve correspondingly has a sharp main peak at 2.16 A and a very broad secondary peak at about twice the distance (4.23 A). There is thus substantial agreement with Maxwell and Mosley's (2) report of "two prominent distances ℓ and 2ℓ" with ℓ equal to 2.13 A.

The necessary information for a detailed demonstration of the trimer structure is clearly not at hand. First of all, there is the possibility that the vapor photographed was a non-equilibrium mixture of evaporated molecular fragments. We have assumed otherwise, however, partly because (A) Professor Brewer has given us his opinion that, under the conditions of the experiment, the vapor from our boiler would probably be predominantly trimeric (the estimated fraction of monomer in the saturated vapor at 450° being only about 4×10^{-5}) (6) and (B), the change in orifice noted in "Experimental" has no perceptible effect on the diffraction pattern. There is also the possibility that the vapor contains a significant fraction of higher polymers - the tetramer has been found in the vapor at 150° (Rosenstock et al; see below), and its presence at higher temperatures is suggested by the negative value for K_2 obtained by Brewer and Lofgren ((1), p. 3040) when they interpreted their data on the reaction of Cu with HCl on the assumption that monomer,

Fig. 1. Visual intensity and radial distribution curves for cuprous chloride. A synthetic radial distribution, plots of interatomic distance vs ∠Cu-Cl-Cu, and a theoretical intensity curve for the alternating, planar, trimeric ring model described in the text.

Fig. 1

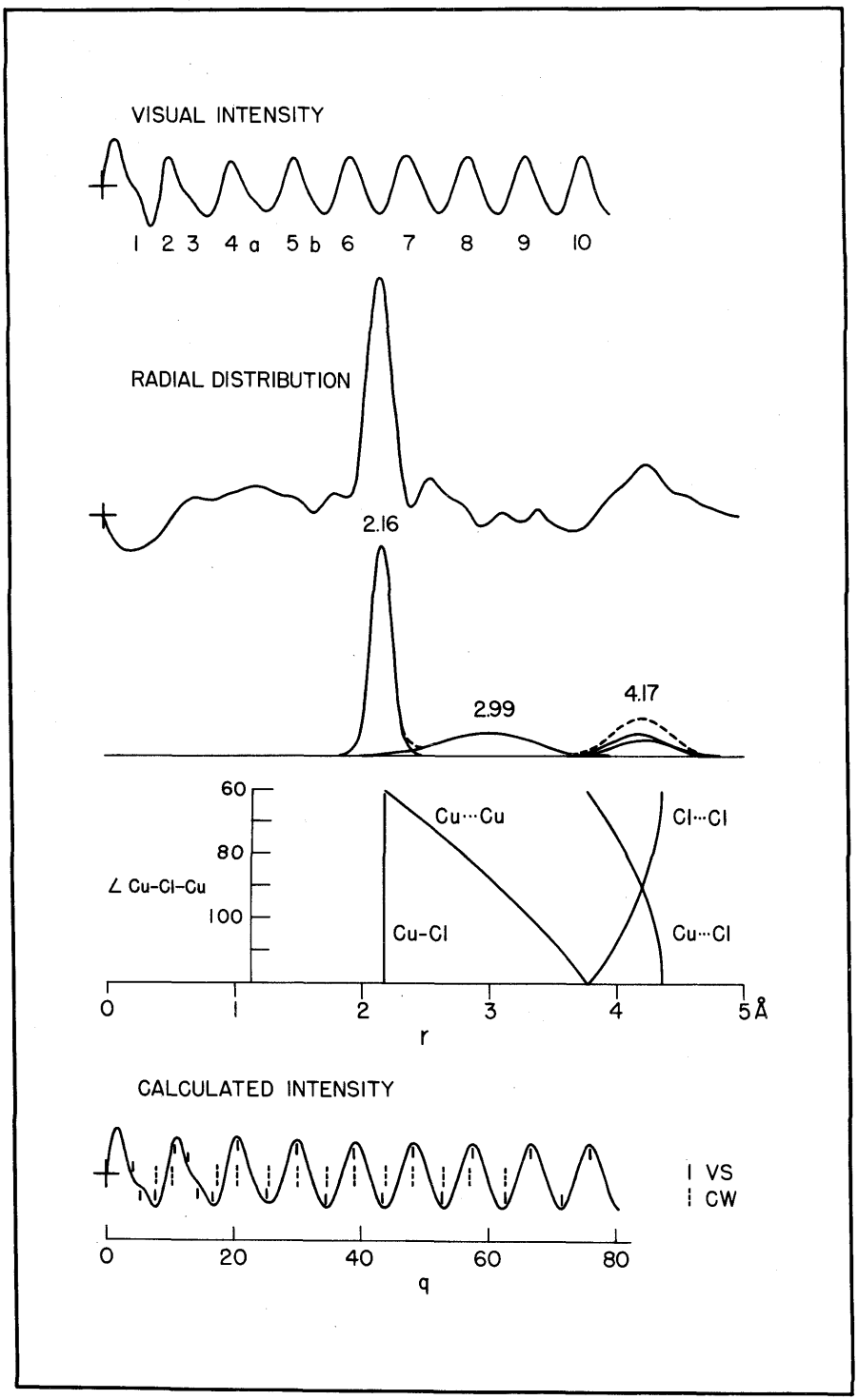
VISUAL INTENSITY
1 2 3 4 a 5 b 6 7 8 9 10
RADIAL DISTRIBUTION
2.16
2.99
4.17
60
80
100
∠ Cu-Cl-Cu
Cu···Cu
Cl···Cl
Cu-Cl
Cu···Cl
0 1 2 3 4 5Å
r
CALCULATED INTENSITY
VS
CW
0 20 40 60 80
q

dimer, and trimer might be present. Nevertheless, we have assumed that our diffraction pattern is due entirely to trimer, and this is probably substantially correct. Even so, more than one model can be made to fit. One that has to be rejected as structurally impossible consists of an equilateral triangle of copper atoms, each bonded to a chlorine atom at about 2.16 A and to two copper atoms, also at about 2.16 A: Cu-Cu = 2.16 A cannot be accepted.

The planar alternating six-ring with large ∠ Cl-Cu-Cl (~150°) and small ∠ Cu-Cl-Cu (~90°) seems the most likely: it has general advantages as cited by Brewer and Lofgren; the bond angles are reasonable*; the great amplitude of symmetric in-plane bending vibration that is required to wash out the unobserved Cu···Cu term suggests that Cu···Cu is a bonding interaction, as suggested by Professor Pauling, but only weakly and only when all three copper atoms are brought together in quasi-metallic fashion**. As may be seen from the plots of distance vs ∠Cu-Cl-Cu in fig. 1, almost any equilibrium angle value will lead to a fit with the radial distribution if the temperature factors are properly adjusted, 90° (or even the complementary 150°) then leading to the greatest conspicuous area above background for the outer peak, whereas larger

---

* In Cu_2O as well as, presumably, other bicoordinate complexes of Cu^+, ∠X-Cu-X is 180°; ∠M-Cl-M is about 90°, the nominal for p^2 bonds, in $PdCl_2$ and many other bicoordinate complexes of Cl^-.

** It could even be suggested that this last aspect of the trimer structure has something to do with its stability relative to the corresponding tetramer, which could have just the ideal bond angles of 90° and 180° but would contain the germ of a different, possibly less stable fragment of metal structure.

or smaller angles, with temperature factors adjusted to emphasize the longer of the distances Cu...Cl and Cl...Cl, center the peak more accurately on the distance 4.23 A. Angles of much less than 80°, however, would imply too short Cu...Cu distances*, or else too narrow a Cu...Cu distribution, and angles greater than about 100° would hardly represent a reasonable approximation to the structural ideals that we have taken as giving support to the ring model. A priori estimates of the vibrational amplitudes would be most helpful but can hardly be made, since we know neither the frequencies nor the actual forms of the several normal modes. We therefore must be content to note that the bending amplitudes quite clearly predominate over the stretching, as expected, and that the symmetrical in-plane bending apparently dominates the asymmetrical, as is made plausible by the argument of quasi-metallic bonding. The relative smallness of the vibrational amplitude for the longest distance in the molecule then invariably follows from the r vs ∠Cu-Cl-Cu plots, which of course describe the relative effects of the symmetrical bending mode. The illustrated theoretical intensity curve** and synthetic distance distribution (drawn with approximate allowance for the artificial temperature factor) and the q_{calc} values for the best rings (Table 1) are for a model with Cu-Cl = 2.16 A,

---

* The shortest Cu...Cu distance in cuprite is 3.01 A, both for inter- and intra-network contacts. In copper itself, Cu-Cu is 2.55 A.

** Various theoretical curves were calculated to test our conclusions from the radial distribution curve.

Table 1

Determination of r_{Cu-Cl} in $(CuCl)_3$

Min.	Max.	$q_{calc.}$[a]	$(q_{calc.}/q_{obs'd.})_{V.S.}$	$(q_{calc.}/q_{obs'd.})_{C.W.}$
	4	20.6	(0.982)	0.999
5		25.6	(1.008)	.994
	5	29.9	0.995	.986
6		34.5	.993	.988
	6	39.1	.999	.996
7		43.7	.999	.988
	7	48.3	.995	.998
8		52.9	.996	.992
	8	57.5	.991	1.003
9		62.1	.983	0.984
		ave_8	0.9939	ave_{10} 0.9928
		a.d.	.0036	.0052

$r_{Cu-Cl} = 2.175 \times 0.9933 = 2.160$ A

---

[a]For model described in text.

$\angle$Cu-Cl-Cu = 87.5°, $\underline{a}_{Cu\cdots Cu} = 1/2\,(\delta \underline{r}^2_{Cu\cdots Cu} - \delta \underline{r}^2_{Cu\text{-}Cl}) = 0.06$ A^2, $\underline{a}_{Cu\cdots Cl} = \underline{a}_{Cl\cdots Cl} = 0.02$ A^2, and $\{(Z - f)_{Cu}/(Z - f)_{Cl}\}_{effective} = 1.3$, as is a fair approximation (7) for the range $0 < q < 20$ of greatest relevance. The theoretical curve is in good agreement with our observations, both of the qualitative aspects ($\underline{a}_{Cl\cdots Cl}$ should probably be reduced somewhat) and, as shown by the arrows, of the ring diameters. The determination of Cu-Cl in Table 1 is substantially independent of the exact choice of angle and $\underline{a}$ values, the temperature factor for all terms except Cu-Cl being so severe. We conclude that Cu-Cl is 2.160 A with limit of error $\pm$ 0.015 A and that the trimer structure is probably the alternating planar six-ring, with $\angle$Cu-Cl-Cu $\sim 90°$ and with a very large amplitude of symmetrical bending vibration.

Discussion. A Cu-Cl distance of 2.16 A corresponds to a Cu radius of 1.17 A, in good agreement with the value of 1.18 A from Cu_2O (8), and considerably shorter than the tetrahedral value, 1.35 A. The difference between the tetrahedral radius and the Ag_2O radius for Ag^+ is similar (8), but we know no other examples for Cu^+*.

Some recent mass spectrometric observations (9) on the cuprous halides seem to tie in with the notion that the copper atoms in $(CuCl)_3$ have a tendency to form a bonded group of some stability. With 75-volt

---

* N. V. Sidgwick ("The Chemical Elements and Their Compounds", Oxford University Press, Oxford, England, 1950, p. 116) in discussing AgCN did not allow for the Ag^+ difference and so was misled into ascribing the correspondingly very large decrement in the observed distance entirely to resonance; $Ag(CN)_2^-$ (p. 134) similarly shows a large decrement.

electrons, the vapor from cuprous chloride held at about 150° produced a main sequence of ions derivable from a parent trimer ion by removal of successive chlorine atoms ($Cu_3Cl_3^+$, $Cu_3Cl_2^+$, Cu_3Cl^+, and Cu_3^+) and weaker sequences of ions containing one, two, or four copper atoms but almost no ions containing more chlorine atoms than copper atoms.

References

1. L. Brewer and N. L. Lofgren, J. Am. Chem. Soc., 72, 3038-45 (1950).

2. L. R. Maxwell and V. M. Mosley, Phys. Rev., 55, 238 (A) (1939).

3. L. R. Maxwell, Abstract American Crystallographic Association Meeting at Pennsylvania State College, April 1950.

4. L. Pauling, Private communication.

5. K. Hedberg and A. J. Stosick, J. Am. Chem. Soc., 74, 954-8 (1952).

6. L. Brewer, Private communication.

7. J. A. Ibers and J. A. Hoerni, Acta Cryst., 7, 405-8 (1954).

8. L. Pauling, "The Nature of the Chemical Bond", Cornell University Press, Ithaca, New York, 2nd Ed. 1940, p. 186.

9. H. M. Rosenstock, J. R. Sites, J. R. Walton and Russell Baldock, J. Chem. Phys., 23, 2442 (1955).

III. Electron Diffraction Study of Molecules Containing Both Light and Heavy Atoms

A. An Electron Diffraction Study of $Pb(CH_3)_4$

Introduction. Early electron diffraction studies led to reports of unequal bond length and hence of low symmetry for uranium hexafluoride and a number of other molecules (also of presumably high symmetry) containing both heavy and light atoms. When the present investigation was begun, these results had just been explained (1) as representing not genuine molecular peculiarity but rather gross error in the atomic electron scattering amplitudes used for the interpretation of the diffraction data. Tests of this explanation for molecules of undoubted symmetry seemed to be in order, and lead tetramethyl was chosen as the first. (An early study (2) of lead tetramethyl, based on inadequate photographs on which only three rings were measured, had failed to reveal any anomaly.) Meanwhile, Ibers and Hoerni (3) have made new calculations of atomic scattering amplitudes, and for these the new photographs provide an important experimental test.

Experimental. The sample of lead tetramethyl (99.8%) was supplied by Dr. G. B. Guthrie, Jr. of the Bartlesville laboratory of the U. S. Bureau of Mines. The photographs were made on Kodak-50 plates in our new apparatus at camera distance 9.627 cm and electron wavelength 0.0618 A; they were interpreted visually in the usual way (4).

Outline of Theory, Results, and Discussion. The diffraction pattern, as represented by the visual curve in fig. 1, is characteristic of compounds having two major terms with approximately equal weight and a few tenths

Legend of Figure 1. Parameters of the calculated curves.

Model*	Pb-C/Pb..H	δ_{Pb-C} (A)	$\delta_{Pb..H}$ (A)	a_{C-C} (A^2)	$a_{Pb..H}$ (A^2)
A	2.21/2.80	0.12	0.15	0.0126	0.006
B	2.21/2.80	0.14	0.15	0.0126	0.006
C	2.21/2.80	0.13	0.15	0.0126	0.006
D	2.21/2.80	0.13	0.15	0.0110	0.006
E	2.21/2.80	0.13	0.15	∞	0.006
F	2.21/2.80	0.13	0.15	0.0126	0.006
G	2.21/2.90	0.13	0.15	0.0126	0.006
H	2.21/2.70	0.13	0.15	0.0126	0.006

* C-H, 1.09 A assumed. D, E, F, G, and H contain no C-H term.

a_{C-H} = 0.00136, assumed.

Fig. 1

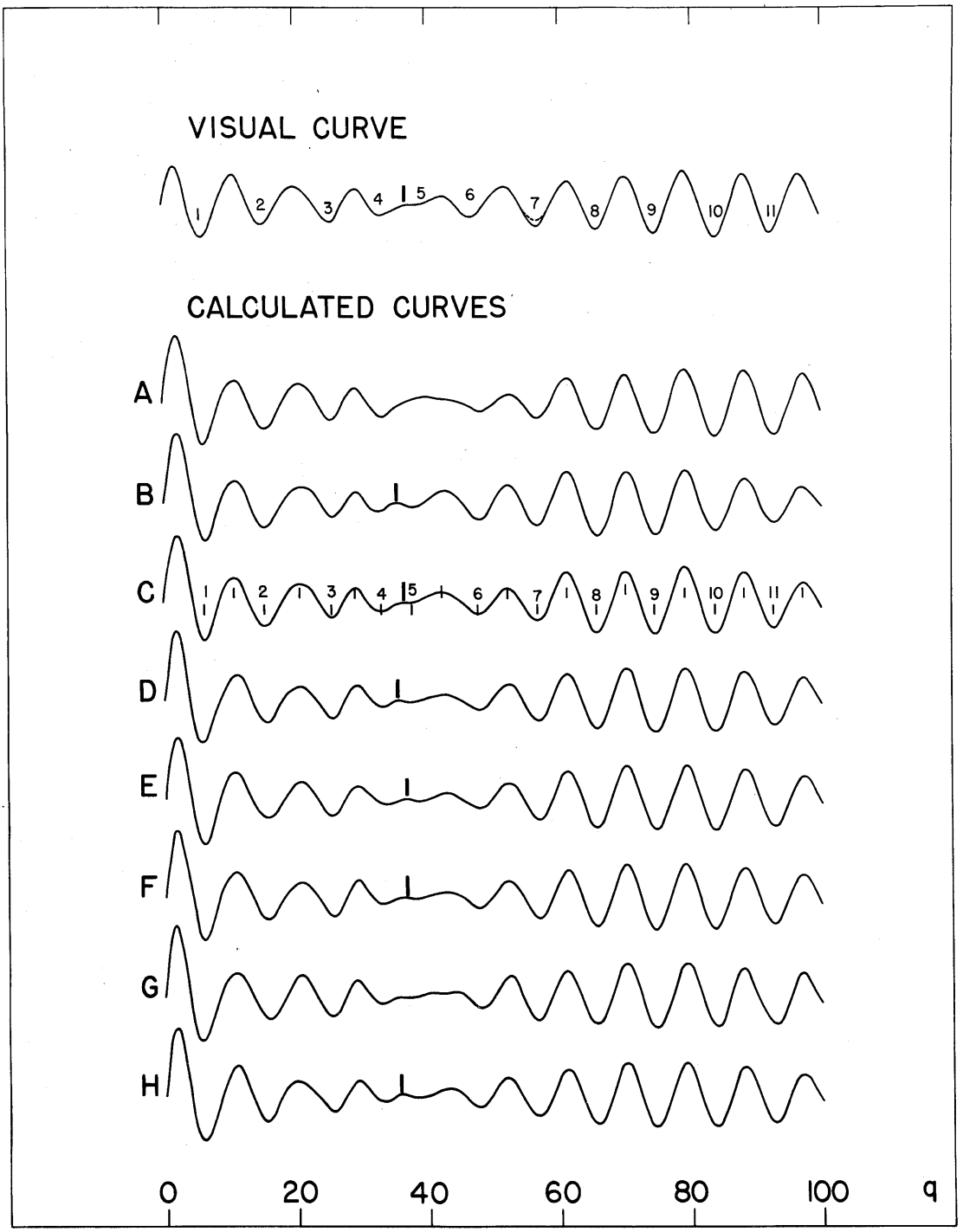
VISUAL CURVE
1
2
3
4
5
6
7
8
9
10
11
CALCULATED CURVES
A
B
C
D
E
F
G
H
0
20
40
60
80
100
q

of an angstrom difference in r. That is, the envelope of the molecular scattering pattern decreases gradually to a minimum at a certain point (defined by the difference in r) and then increases again. The conventional interpretation would accordingly be that there are two pairs of different Pb-C bond lengths in the $Pb(CH_3)_4$ molecule. However, this conclusion is just as erroneous as many other early electron diffraction conclusions on compounds containing both heavy and light atoms, such as UF_6, OsO_4, etc., in that the heavy-light interatomic distances in each compound were reported to be unequal, contrary to all the other physical chemical observations. These anomalous results of electron diffraction, as explained by Schomaker and Glauber (1), were a consequence of using, even for heavy atoms, the atomic scattering factor obtained from the Born approximation - the Born approximation is limited to small Z and λ. The true atomic scattering factor for electron diffraction is a complex quantity, $f = |f| \exp(i\eta)$, where both $|f|$ and η, the phase angle, are functions of Z, s, and λ. The usual intensity function then becomes

$$sI(s) = k\sum_{ij} f_i f_j^* \frac{\sin r_{ij}s}{r_{ij}} = k\sum_{ij} |f_i||f_j| \cos(\Delta\eta)_{ij} \frac{\sin r_{ij}s}{r_{ij}}.$$

The amplitude of the (i,j) term reaches zero at a point $s_{0,ij}$, the cut-off point, where the difference $\Delta\eta_{ij}$ of the phase angles of f_i and f_j reaches $\pi/2$. Thereafter, the amplitude changes sign. This seems to account for the observed anomaly rather well. A single 'heavy-light'

term $|f_i|\,|f_j|\cos(\Delta\eta)_{ij}\frac{\sin\Lambda_{ij}s}{\Lambda_{ij}}$ of sI(s) is roughly equivalent to a pair of ordinary terms with coefficients $\frac{1}{2}|f_i||f_j|$ and distance values, $(r + \Delta r/2)_{ij}$ and $(r - \Delta r/2)_{ij}$. The difference Δr_{ij} of the two virtual distances is referred to as the 'apparent split'; it is given to a good approximation by $(\Delta r \cdot s_o)_{ij} = \pi$.

In this investigation, the atomic scattering amplitudes $|f_i|$ were used for all the atoms just as given by Ibers and Hoerni (3), but their phase angle differences were varied somewhat. The intensity function was appropriately modified, as described in Appendix I, for convenience of calculation by our routine punch-card method (5).

A few of the calculated curves, as shown in fig. 1, demonstrate the sensitivity of the diffraction pattern to variation of the critical parameters. It turns out that in the region near the expected Pb-C cut-off point ($q \sim 38$), the pattern is extremely responsive to almost all the parameters. As an outstanding example, maximum 4, indicated by heavy bars in fig. 1., is a very sharp although rather weak feature. To fit maximum 4 to its observed position and shape, the cut-off points of both Pb-C and Pb.H have to be moved about 10% from the calculated value (3) (curves A, B, and C), and the temperature factors of C.C and Pb.H have to be critically adjusted (curves C, D, and E). The resulting temperature factors are consistent with the observed vibrational frequencies (6).

The C-H term, as expected, does not play an important role in this determination (curves C and F). Our data also provide a determination of the Pb.H distance (curves G and H). Curve C, based on our best model (Table 1), is in excellent agreement with the visual curve.

Table 1

Measured and calculated q values of Model C

Max.	Min.	$(q_o)^1$	(q/q_o)	w
	1	6.08	1.020	0
1		11.07	0.967	0
	2	15.55	.990	1
2		19.96	1.032	0
	3	25.79	.988	2
3		29.44	0.988	5
	4	33.21	1.000	2
4		36.90	0.989	0
	5	39.92	0.952	0
5		43.66	0.971	1
	6	47.64	1.003	1
6		52.68	0.993	2
	7	57.42	0.990	5
7		61.66	0.993	10
	8	65.88	0.997	10
8		70.40	.996	10
	9	74.81	1.000	10
9		78.57	1.008	5
	10	(83.31)	1.006	5
10		(88.09)	1.001	2
	11	(91.89)	1.009	2
11		(97.27)	0.998	1

[1] Ave. of C.W. and V.S.
( ) V.S. only.

Table 1 (Cont'd)

Weighted mean = 0.9970 (scale factor)

Δr_{Pb-C} = 0.26 ± 0.01 A

$\Delta r_{Pb..H}$ = 0.30 ± 0.03 A

Pb-C = 2.21 x 0.9970 = 2.203 ± 0.010 A

Pb..H = 2.80 x 0.9970 = 2.79 ± 0.050 A

($\angle$ H-C-Pb = 109.0 ± 4.0°)

The apparent splits determined, 0.26 A for Pb-C, and 0.30 A for Pb-H, are in fair agreement with the calculated values (3) 0.279 A for Pb-C and 0.331 A for Pb.H. The Pb-C bond length, 2.203 A, is in excellent agreement with Pauling's covalent radius for quadrivalent lead, 1.430 A (7), which leads to the value 2.200 A for Pb-C. The early electron diffraction value, 2.29 $\pm$ 0.05 A (2), is quite incompatible with our result. The Pb.H distance, 2.79 A, the Pb-C distance, 2.203 A, and the assumed C-H distance, 1.09 A, define the value 109.0° for $\angle$ H-C-Pb.

Appendix I

A familiar form of the molecular scattering function appropriate for correlation with the visually estimated intensity for $Pb(CH_3)_4$ is

$$sI(s) = \frac{4}{r_{Pb\text{-}C}} \frac{|f_{Pb}||f_C|}{\sum_i |f_i|^2} \cos(\Delta\eta)_{Pb\text{-}C} \sin r_{Pb\text{-}C}\, s$$

$$+ \frac{12}{r_{Pb\cdots H}} \frac{|f_{Pb}||f_H|}{\sum_i |f_i|^2} \cos(\Delta\eta)_{Pb\cdots H} \exp(-a_{Pb\cdots H} s^2) \sin r_{Pb\cdots H}\, s$$

$$+ \frac{6}{r_{C\cdots C}} \frac{|f_C|^2}{\sum_i |f_i|^2} \exp(-a_{C\cdots C} s^2) \sin r_{C\cdots C}\, s$$

$$+ \frac{12}{r_{C\cdots H}} \frac{|f_C||f_H|}{\sum_i |f_i|^2} \cos(\Delta\eta)_{C\text{-}H} \exp(-a_{C\cdots H} s^2) \sin r_{C\cdots H}\, s,$$

where $\sum_i |f_i|^2$ may be approximated as $|f_{Pb}|^2$.

For convenience in punch-card calculation, the function

$$I(s) = \frac{2}{r_{Pb\text{-}C}} \left\{ \sin (r+\delta)_{Pb\text{-}C}\, s + \sin (r-\delta)_{Pb\text{-}C}\, s \right\}$$

$$+ \frac{6}{r_{Pb\cdots H}} \phi \exp(-a_{Pb\cdots H} s^2) \left\{ \sin (r+\delta)_{Pb\cdots H} s + \sin (r-\delta)_{Pb\cdots H}\, s \right\}$$

$$+ \frac{6}{r_{C\cdots C}} \psi \exp(-a_{C\cdots C} s^2) \sin r_{C\cdots C} s + \frac{12}{r_{C\cdots H}} \omega \exp(-a_{C\cdots H} s^2) \sin r_{C\cdots H}\, s,$$

where

$$\gamma = \{(\cos \delta_{Pb\text{-}e}\, s)|f_c|\} \,/\, \{(\cos \Delta\eta_{Pb\text{-}e})|f_{Pb}|\},$$

$$\phi = \{(\cos \Delta\eta_{Pb\text{-}H} \cos \delta_{Pb\text{-}e}\, s)|f_H|\} \,/\, \{(\cos \Delta\eta_{Pb\text{-}e} \cos \delta_{Pb\text{-}H}\, s)|f_c|\},$$

$$\omega = \{(\cos \Delta\eta_{e\text{-}H} \cos \delta_{Pb\text{-}e}\, s)|f_H|\} \,/\, \{(\cos \Delta\eta_{Pb\text{-}e})|f_{Pb}|\},$$

and $\delta_{ij} = \frac{1}{2}\Delta\eta_{ij}$ was evaluated instead.

For the range of interest, γ, ϕ, and ω are approximately constant except for q less than 15 (in the region for q less than 15, Gaussian approximations may be used for γ, ϕ, and ω).

The functions γ, ϕ and ω were approximated as constants in this investigation. If the variations of the cut-off points were assumed to be due to changes in the scale factor of cos $\Delta\eta$'s only (i.e., the shape of cos $\Delta\eta$'s are invariant), the constant approximations for γ, ϕ and ω would hold for all the variations of s_o's illustrated.

B. An Electron Diffraction Investigation of CF_3I

Introduction. This is the second of a series of electron diffraction studies of molecules containing both light and heavy atoms. The background of these investigations will not be repeated here since it has already been given in IIIA, on $Pb(CH_3)_4$. The major purpose is to test Hoerni and Ibers' calculation on the complex atomic scattering factors for electron diffraction (3), but the structure of CF_3I is itself also of definite interest.

Although the structure of CF_3I has already been studied both by the microwave method (8) and by electron diffraction (9), the reported results are hardly satisfactory. In the microwave investigation, only a single function connecting the three structural parameters was determined. In the electron diffraction work the gross errors in phase of the usual atomic scattering factors were not noticed, perhaps because only rather limited data ($q_{max} \sim 75$) were obtained, and the final parameters were evaluated in a strange way.

Experimental. Both sector photographs (Kodak process plates) and non-sector photographs (Kodak 50 plates) were made ($\ell \sim 10$ cm, $\lambda \sim .06$ A)*, and the diffraction pattern was interpreted visually in the usual manner (4).

---

* ℓ = 9.627 cm.

λ = 0.0623 A, average for sector photographs and the first-set non-sector photographs, for calculation of q_o's.

λ = 0.0627 A, average for sector photographs.

λ = 0.0619 A, average for the first-set non-sector photographs.

There are two sets of non-sector photographs. One set made in 1954 with a sample prepared by C.W., is fairly good ($q_{max} \sim 80$) but possibly does not include pictures as heavy as might have advantageously been taken. The other set, taken concurrently with the sector photographs in 1956 with a sample obtained from the Caribou Chemical Company, is very poor ($q_{max} < 50$) because only out-dated plates were available at the time. However, the sector photographs provide us with good data to $q \sim 100$, and with observable features all the way to the edge of the sector ($q \sim 150$). The features beyond $q = 100$ are rather diffuse and therefore difficult to measure and interpret accurately; they are given reduced weight. The features between $q = 33$ to $q = 46$ are very elusive on the non-sector photographs, especially maximum 6, which amounts to only about 0.1% of the total scattering and is very difficult to locate and describe accurately. The sector photographs are very clear in that region; however, sector imperfections (the calibration curve, plotted as $\frac{i^3}{\alpha}$, has a rather sharp peak at about $q = 46$ amounting to 1.6% of $\frac{i^3}{\alpha}$, and a smaller sharp peak at $q = 38$) completely invalidate this region of the sector pictures. Therefore, the best we can say is that some models are closer to what we observe on the non-sector photographs than the others.

Results and Discussion. The molecular scattering pattern, as represented by the visual curves in fig. 2*, begins with several simple

---

* Curve C.W. - At first, the non-sector photographs were used for interpretation of features within $q = 33$ only, and the sector photographs for $q > 22$. Later, the imperfection of the sector was noticed; the necessary corrections of the visual curve are significant between $q = 36$ and $q = 53$. A reexamination of the non-sector photographs confirmed this error. The revised curve is indicated by the dashed line.

Legend to Fig. 2

Curves	$\frac{CI}{CF}$	$\angle$ F-C-F	δ_{FI} (A)	δ_{CI} (A)	a_{FI} $10^4 A^2$	a_{CI} $10^4 A^2$	a_{FF} $10^4 A^2$
B	1.617	107.5	.08	.08	10	5	5
C	1.629	108.5	.08	.08	20	16	16
C_1	"	"	.09	.10	20	16	16
E	1.579	"	.08	.08	10	5	5
G	"	106.5	.08	.08	10	5	5
I	1.598	107.5	.08	.08	10	5	5
L	1.629	109.5	.08	.08	20	16	16
L_1	"	"	.07	.07	20	16	16
N	1.594	108.5	.08	.08	10	5	5
N'	"	"	.09	.094	10	5	5

Fig. 2

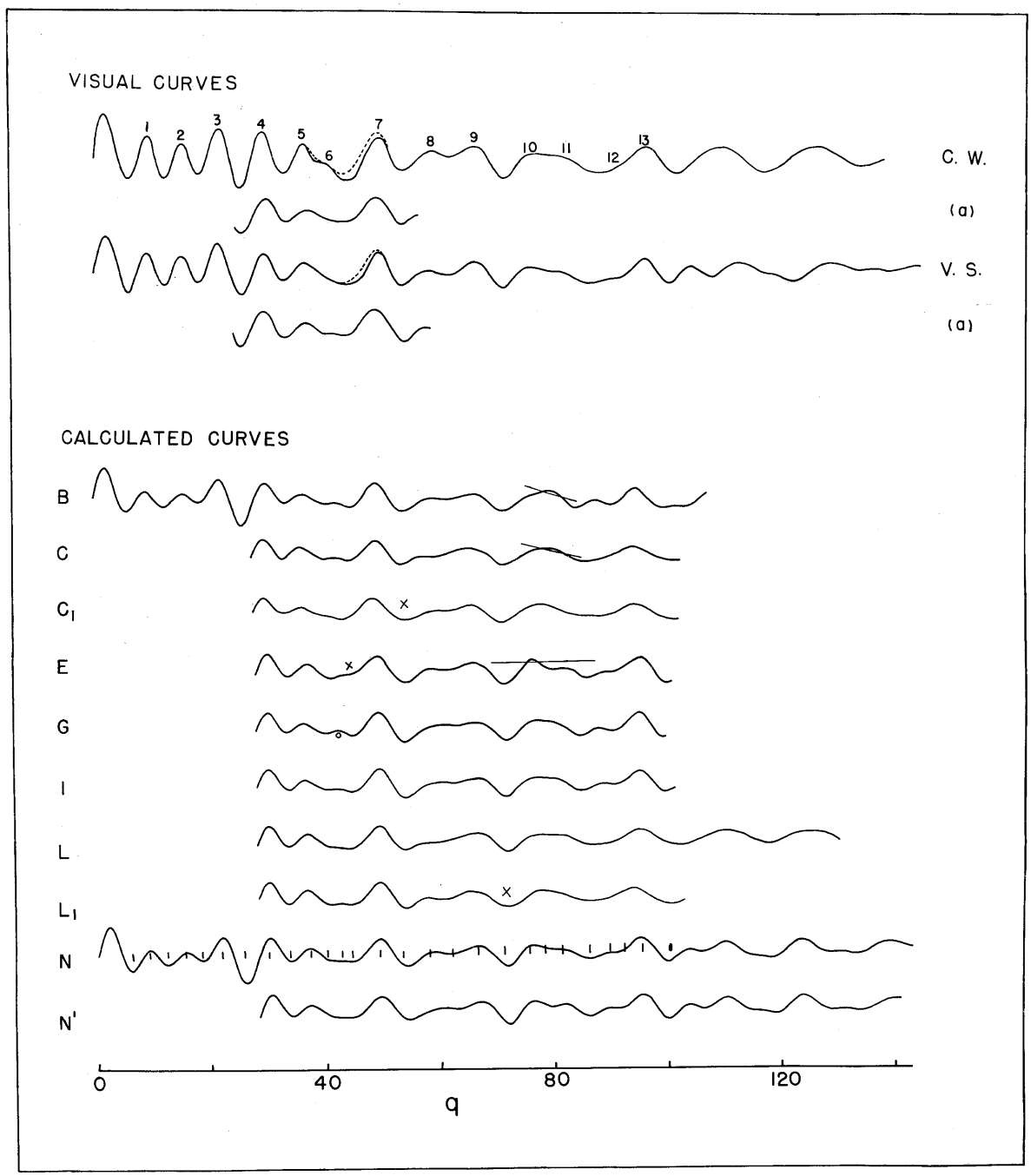
VISUAL CURVES
1
2
3
4
5
6
7
8
9
10
11
12
13
C. W.
(a)
V. S.
(a)
CALCULATED CURVES
B
C
C1
E
G
I
L
L1
N
N'
0
40
80
120
q

rings, then develops into a series of complicated features, and finally becomes somewhat simple again near the limit of the present observations.

The pattern is indeed complicated and at least eight parameters of the molecular model and the scattering theory enter into its interpretation: the size parameter, the two shape parameters, three differential vibration parameters, and two phase-shift parameters of the kind defined in IIIA to describe the most important possible changes in the scattering phase angles.

A number of theoretical intensity curves were calculated, based on models comparable to both the RDI (not shown) and the microwave data (8). The complex atomic scattering factors given by Hoerni and Ibers (3) were used for all atoms, but were modified for most of the curves by varying the two phase-shift parameters.

The I-F cut-off point, $q_{o,IF}$, was primarily determined by the shapes of maxima 8 and 9 and minima 8 and 10. For a good fit to the visual curve, the F-I cut-off point has to be close to $q \sim 60$. Maxima 8 and 9 and minima 8 and 10 are relatively insensitive to all the other parameter variations illustrated. Moving the I-F cut-off point inside

---

(Cont'd from previous page)

Curve V.S., at first was drawn as a compromise of the observations on sector and the non-sector photographs for q, 36-53. Although the rather striking difference in appearance of features in this region between the non-sector photographs and the sector photographs was noticed, V.S., failing to consider the by then known sector calibration curve, became convinced that the difference was not so great as it at first seemed to be (and we now know, is) and that further, the original sample may have been impure (as, we may now assume, it was not). Since the original interpretation in the region $36 < q < 53$ is a compromise, the correction, in dashed line, is not as large as C.W.'s.

Curves C.W.(a) and V.S.(a) - New interpretation based on first set non-sector photographs only.

$q \sim 52$ results in broadening minimum 8 and shifting maximum 8 outward away from the observed position. Moving the I-F cut-off point outside $q \sim 67$ broadens minimum 10 and weakens and deforms maximum 9. The best choice is perhaps $q_{o,FI} = 59$. The I-C cut-off point is less well determined; it is effectively coupled with a_{I-C} and $r_{F.F}$. For a reasonable a_{I-C}, for the range of $r_{F.F}$ fixed below, and for the theoretical calculations (3), (10), (11), which predict that $q_{o,CI} < q_{o,FI}$, $q_{o,CI} = 55$ seems best. Curves C, L, N and N', illustrating the effects of several variations of $q_{o,FI}$ and $q_{o,CI}$, may be used to follow the above description.

The shape parameters (C-I/C-F and F-C-F) for $q_{o,FI} = q_{o,CI} = 62.5$ (space A) and for $q_{o,FI} = 55.5$ and $q_{o,IC} = 53$ (space B) were thoroughly investigated.

The shape parameters for space A are determined by the following considerations.

Maximum 6 grows larger toward curves D*, B, I, G and A*, and moves into maximum 7 in curves E and F*. The three-fold comparison that maximum 10 is below the average of maxima 9 and 13 fails in curves D*, E and F*. The feature that maximum 11 is lower than maximum 10 is not reproduced in curves A*, B, C, L and H*. The position of minimum 9 is very much shifted toward maximum 9 in curve G. Thus, curves A, B, C, D, E, F, G and H define the range of acceptability of the shape parameters (fig. 3). For curves inside the range, good agreement with the visual curves is obtained as shown by curves L, I and N.

---

* Not illustrated in fig. 2.

The shape parameters for space B are determined with somewhat similar considerations with the addition of the shape of minimum 8 which is more sensitive to shape parameters in this space. The range of acceptability illustrated in fig. 3 is very much smaller.

Limits of acceptability for the size parameter ($(r_{C-F})_c$ · scale factor)* were determined with the help of microwave information (8). For each model, the resulting C-F bond length has an estimated range of uncertainty of about ± 0.01 A, and models for which r_{C-F} deviates more than 0.01 A from that indicated by the microwave data are considered as unacceptable. The range of acceptability for the size parameter in space A was then defined for the portion of interest by models G, I, J, and L (fig. 3) and in space B, by models Q', I', K', and H' (fig. 4).

The temperature factors are not very critical in this investigation. The values we accepted as feasible, $a_{I.F} = 0.0010\ A^2$,** $a_{F.F} = 0.0005\ A^2$, and $a_{I-C} = 0.0005\ A^2$, ($a_{XY} = (\bar{\delta}r^2_{XY} - \bar{\delta}r^2_{C-F})/2$) seem to be at least roughly compatible with the spectroscopic data (12).

The final model (Table 2) was interpolated from the best models in space A and space B***. The best model in either space was interpolated from all the acceptable models (models inside the overlapping area of the range of acceptability of the shape parameters and the range of acceptability of the size parameter) with consideration given to the over-

---

* The scale factor was the average of q_c/q_o of six well distributed and distinguished features: minima 5, 8 and 10 and maxima 7, 9 and 13.

** $a_{I.F}$ is critical for the fine structures beyond q = 100 in V.S. visual. Compare curves L and N.

*** The X in fig. 3 and fig. 4.

Legend to Fig. 3 and Fig. 4

——— Microwave contour

– – – Approximate electron diffraction contour

▬▬ Range of acceptability of the shape parameters

▪▪▪ Range of acceptability of the size parameter

▪▬▪ Estimated boundary for the range of acceptability of the size parameter

X Best model

Model	$(r_{C-F}$ S.F.$)^{*,a}$ (A)	Model	$(r_{C-F}$ S.F.$)^{*,a}$ (A)
B	1.341	B'	1.338
C	1.329	C'	1.332
D	1.351	D'	1.350
E	1.346	E'	1.347
F	1.338	F'	1.341
G	1.349	G'	1.347
H	1.327	H'	1.330
I	1.344	I'	1.344
J	1.338	K'	1.334
K	1.334	M'	1.344
L	1.331	N'	1.344
M	1.345	Q'	1.346
N	1.342		
P	1.342		

* S.F. - scale factor

a The ave. dev. of S.F. is within the range of .004 - .008

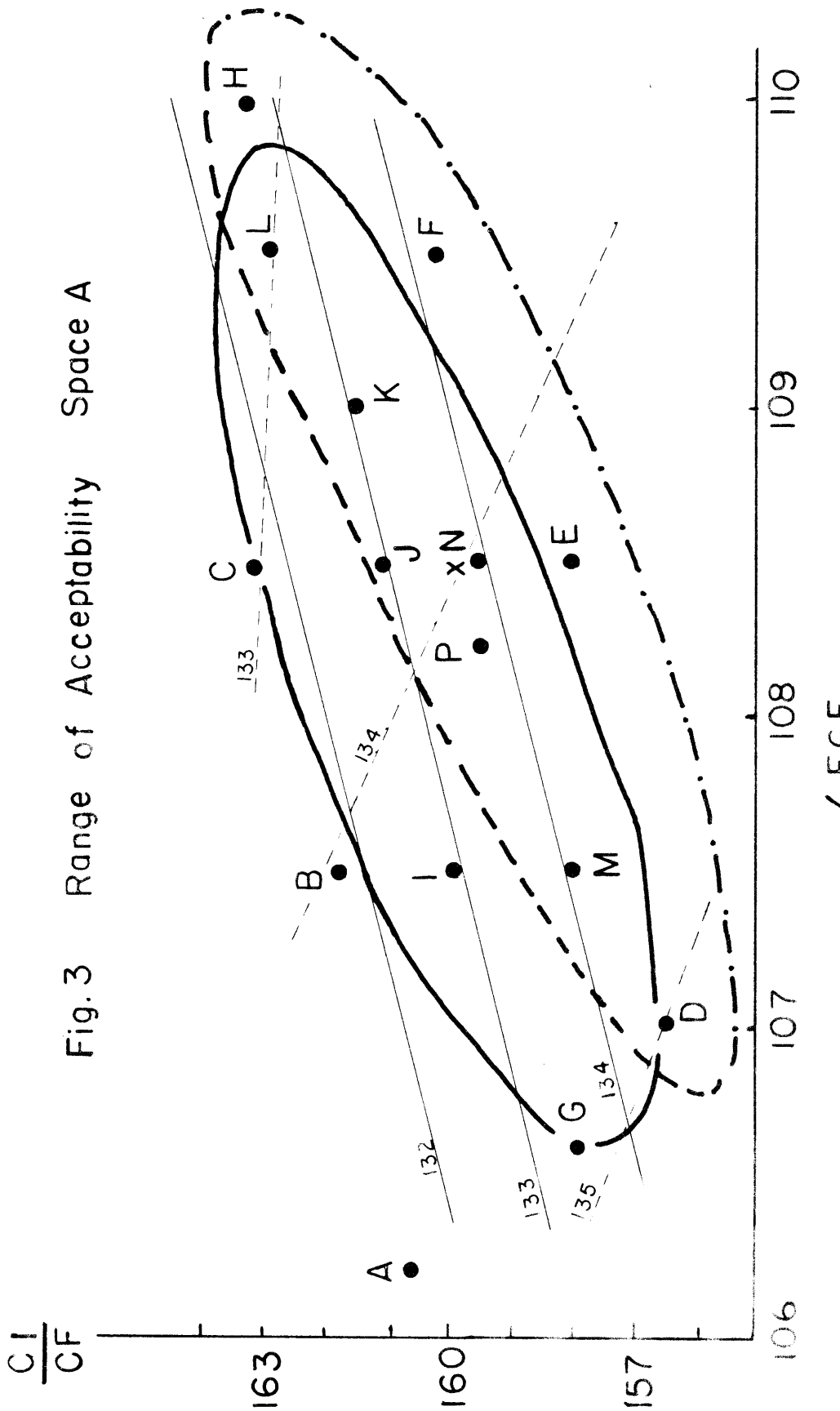

Fig. 3 Range of Acceptability Space A

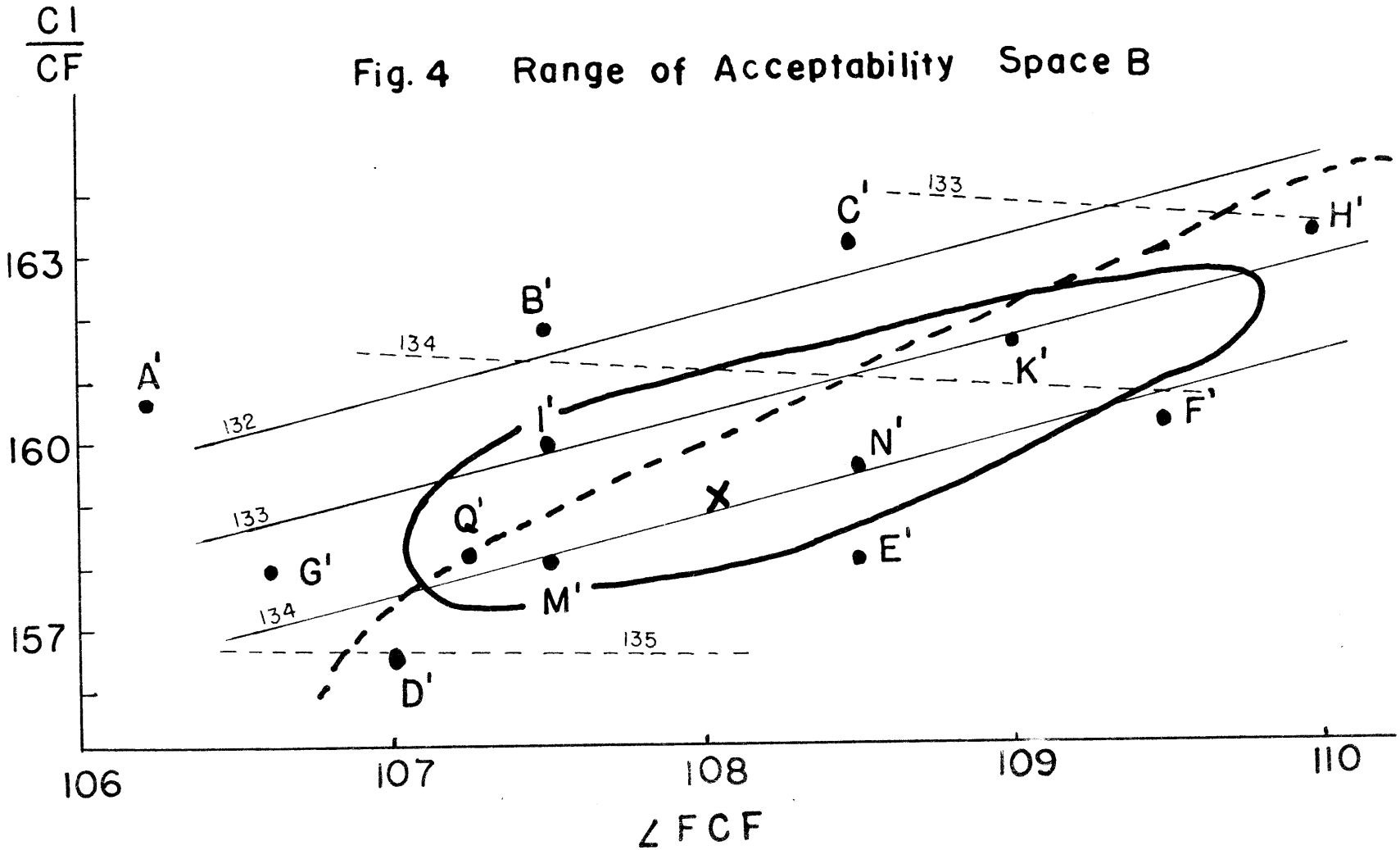

Fig. 4 Range of Acceptability Space B

Table 2

Min.	Max.	$10^2(q_o)_{av}$	$10^3(q_c/q_o)$ (N)[a]	$10^3(q_c/q_o)$ (N')[a]
1		622[c]	949[b]	949[b]
	1	913[c]	997[b]	997[b]
2		1210[c]	1017[b]	1017[b]
	2	1512[c]	1025[b]	1020[b]
3		1812	1010	1001
	3	2150	1023	1009
4		2536[d]	1021	1025
	4	2979[d]	1014	1007
5		3347[d,*]	1007	1007
	5	3729[d]	981	987
6		4010[d]	997[b]	1012[b]
	6	4265[d]	1001[b]	996[b]
7		4435[d]	1003[b]	1003[b]
	7	4935[d,*]	1001	999
8		5333*	1016	1022
	8	5790	1014	1019
9		6207	994	1015
	9	6645*	1007	1008
10		7100*	1010	1007
	10	7534	1012	1004
11		7804	1015	1010
	11	8123	1006	1007
12		8601	1000	996
	12	8953	1000	997
13		9210	991	994
	13	9532*	999	1000
14		10041	994	1004
	Ave. (20)		1006	1006
	Ave. dev. (20)		.0076	.0071

Table 2 (Cont'd)

Final results

$r_{C-F} = 1.342 \pm 0.015$ A

$r_{C-I} = 2.134 \pm 0.025$ A

$\angle F\text{-}C\text{-}F = 108.3 \pm 1.5^{\circ}$

$(q_o)_{I..F} = 59.0 \pm 5.0$

$(q_o)_{I-C} = 55.0 \pm 8.0$

---

a Represent the best models in space A and space B

b Not included in the average

c C.W. only

d V.S. measurement on first set non-sector photographs only

* For scale factor calculation

all agreement in shapes and positions of the features of the calculated curves as compared with the observations. Similar considerations were used to deduce the final model.

The accepted value of the cut-off points are in good agreement with the calculated value q = 57.5 for F·I and q = 51.0 for C-I. The C-F bond length and ∠F-C-F bond angle determined in this investigation are comparable to those existing values for trifluoromethyl derivatives such as: CF_3Cl (E.D. ∠F-C-F, 108.6 ± 0.4°; C-F, 1.328 ± 0.002 A) (13), $HCCCF_3$ (m.w. and E.D., ∠F-C-F, 107.5 ± 1.0°; C-F, 1.335 ± 0.01 A) (14), CF_3H (m.w., ∠F-C-F, 108.48°; C-F, 1.332 A) (15), etc. The C-I bond length is also in the range of those reported values: 2.12 ± 0.02 A and 2.15 ± 0.015 A for CI_4 (E.D.) (15), 2.14 ± 0.04 A for CH_2I_2 (E.D.) (15), 2.12 ± 0.04 A for CHI_3 (E.D.) (15) and 2.139 A for CH_3I (m.w.) (16).

C. A Brief Comment on the Results of IIIA and IIIB on Atomic Scattering Factors for Electron Diffraction

The experimental results of the electron diffraction study of $Pb(CH_3)_4$ (IIIA) and CF_3I (IIIB) at 40 kev have verified conclusively the complex nature of the atomic scattering factor as pointed out by Schomaker and Glauber (1). Although three sets of calculations on the complex scattering factors are available, Glauber-Schomaker's (second Born approximation with screened coulumb potential) (10), Glauber's (more refined calculation with screened coulumb potential) (11) and Hoerni-Ibers' (partial wave solution with Thomas-Fermi potential) (3), the result of Hoerni-Ibers' calculation was chosen as a basis for these investigations in view of the previous result on UF_6 at 10 kev (17) which ruled out the first two.

As described in IIIA and IIIB, the experimentally determined cut-off points are in pleasing agreement with those predicted from the Hoerni-Ibers' scattering phase angles (usually within 10%). The amplitudes of the atomic scattering factors are usually not very sensitive in this kind of work; however, we feel that both f^B and Hoerni-Ibers' |f| will do. The conventional approximation, Z, is quite unsuitable for light-heavy compounds. We found that in the case of CF_3I, the Z approximation would give a clearly distinguished maximum 6, completely contrary to our observation.

All in all, despite the use of the Thomas-Fermi potential for light atoms and the neglect of valence distortion, the Hoerni-Ibers'

calculation of atomic scattering factors for electron diffraction has already passed the severe test and has proved to be essential, with some modification of $\Delta\eta$'s, for studying the structures of light-heavy compounds.

References

1. V. Schomaker and R. Glauber, Nature, 170, 290-1 (1952).
2. L. O. Brockway and H. O. Jenkins, J. Am. Chem. Soc., 58, 2036-44 (1936)
3. J. A. Ibers and J. A. Hoerni, Acta Cryst. 7, 405-8 (1954).
4. K. Hedberg and A. J. Stosick, J. Am. Chem. Soc., 74, 954-8 (1952).
5. P. Shaffer, V. Schomaker and L. Pauling, J. Chem. Phys., 14, 659-64 (1946).
6. C. W. Young, J. S. Koehler and D. S. McKinney, J. Am. Chem. Soc., 69, 1410-5 (1947).
7. L. Pauling, Proc. Roy. Soc. A, 196, 343-62 (1949).
8. J. Sheridan and W. Gordy, J. Chem. Phys. 20, 591-5 (1952).
9. H. J. M. Bowen, Trans. Faraday Soc., 50, 444-51 (1954).
10. R. Glauber and V. Schomaker, Phys. Rev., 89, 667-71 (1953).
11. R. Glauber, private notes; rough formulation is available in J. A. Ibers' Ph.D. Thesis, California Institute of Technology, 19-25 (1954).
12. S. R. Polo and M. K. Wilson, J. Chem. Phys., 20, 1183 (1952).
13. L. S. Bartell and L. O. Brockway, J. Chem. Phys., 23, 1860-2 (1955).
14. J. N. Shoolery, R. G. Shulman, W. F. Sheehan, V. Schomaker and D. M. Yost, J. Chem. Phys., 19, 1364-9 (1951).
15. P. W. Allen and L. E. Sutton, Acta Cryst., 3, 46-72 (1950).
16. S. L. Miller, L. C. Aamodt, G. Dousmanis, C. H. Townes and J. Kraitchman, J. Chem. Phys., 20, 1112-4 (1952).
17. J. A. Hoerni and J. A. Ibers, Phys. Rev. 91, 1182-85 (1953).

IV.* Electron Diffraction Investigations of Two Polycyclohydrocarbons - Norbornane and the Compound $C_{12}H_{14}$ of De Vries and Winstein

---

* The work described in this section was done in collaboration with Mr. A. Berndt.

Fig.1

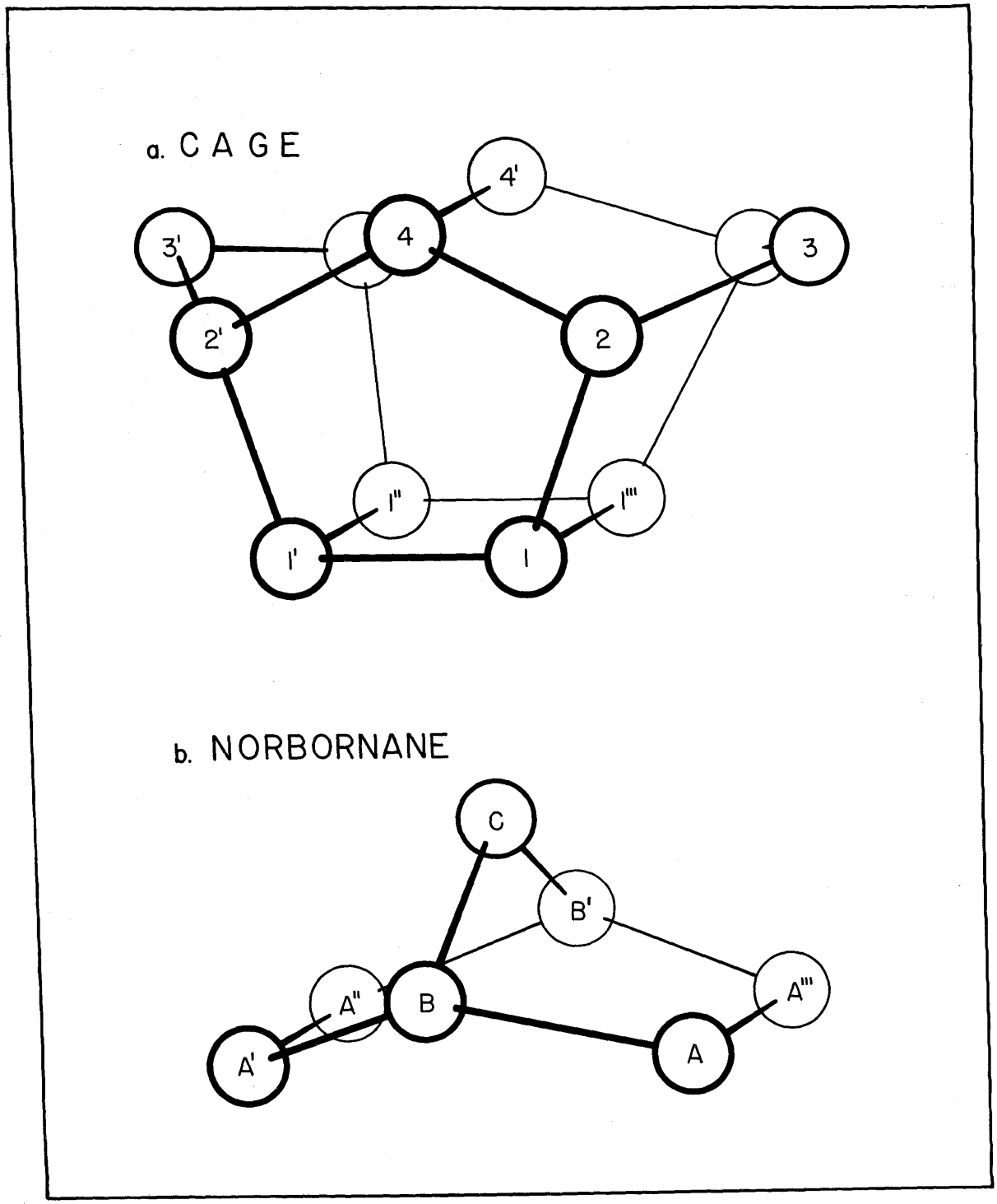

Introduction. The compound $C_{12}H_{14}$ was synthesized by De Vries and Winstein at UCLA (1). They proposed a structural formula (fig. 1a) based solely on the method of preparation. Because of its cage-like appearance and for lack of a more suitable name, we have called it the "cage". Initial x-ray crystallographic work on this compound failed to yield a structure because of rotation of the molecule in the crystal (2), and a low temperature study has as yet not been seriously attempted. Therefore, in spite of the formidable number of parameters, it was felt that a careful electron diffraction study would provide a useful test of De Vries and Winstein's model and would provide information on bonding in polycyclic systems.

The preliminary measurements indicated an unexpected lengthening of the average C-C single bond (see later text) from its normal value of 1.54 A. This result drew our attention to the effect of cross-ring repulsion which has been considered to be the main cause of lengthening of the C-C single bond in cyclobutane (3). At this time Professor Winstein agreed that an investigation of norbornane (bicyclo 2,2,1 heptane, (fig. 1b)), a compound of known structural formula which has similar structural features with the proposed cage model, would be useful, and he supplied the necessary impetus by giving us a sample.

In the study of the related compound nortricyclene (4), the possible lengthening of the C-C bond in the five-membered rings was masked by the interactions between the C-C bonds in the cyclopropane and cyclopentane rings.

The experimental work is an attempt to answer the following questions: Does the cage really have structural features similar to norbornane? What can be said in detail about the structures of the cage and norbornane? Is the C-C bond length in norbornane also stretched?

Experimental. Diffraction photographs (Kodak 50 plates) were taken of the cage and norbornane* ($\lambda \sim 0.06$ A , $\ell \sim 10$ cm). The diffraction patterns were interpreted visually in the usual manner (5).

Results and Discussion. The visual curves (fig. 2)** for the cage and norbornane exhibit many similar features, although the pattern of the cage shows the more pronounced high frequency terms. The radial distribution curves (RDI)*** for both molecules have two similar main

---

* Sample-bulb temperatures:
Cage $\sim$ 115°C
Norbornane $\sim$ -10°C

** Curves A (Cage), V.S.
Curves B (Norbornane), C.W.
All three investigators independently examined the plates and they agreed on the main features of both compounds. However, in the case of the cage, A.B. and C.W. overlooked several fine features of the pattern because of inexperience and in addition the curve of A.B. suffers from several exaggerations. Curve V.S. extends to larger q values. For norbornane curve A.B. suffers the same shortcomings as above, while C.W. and V.S. are in excellent agreement except for two features. The dashed lines in fig. 2 show the interpretation by V.S. for these two features.

*** Distances for the cage beyond 4 A are not shown on the RDI.

Fig. 2

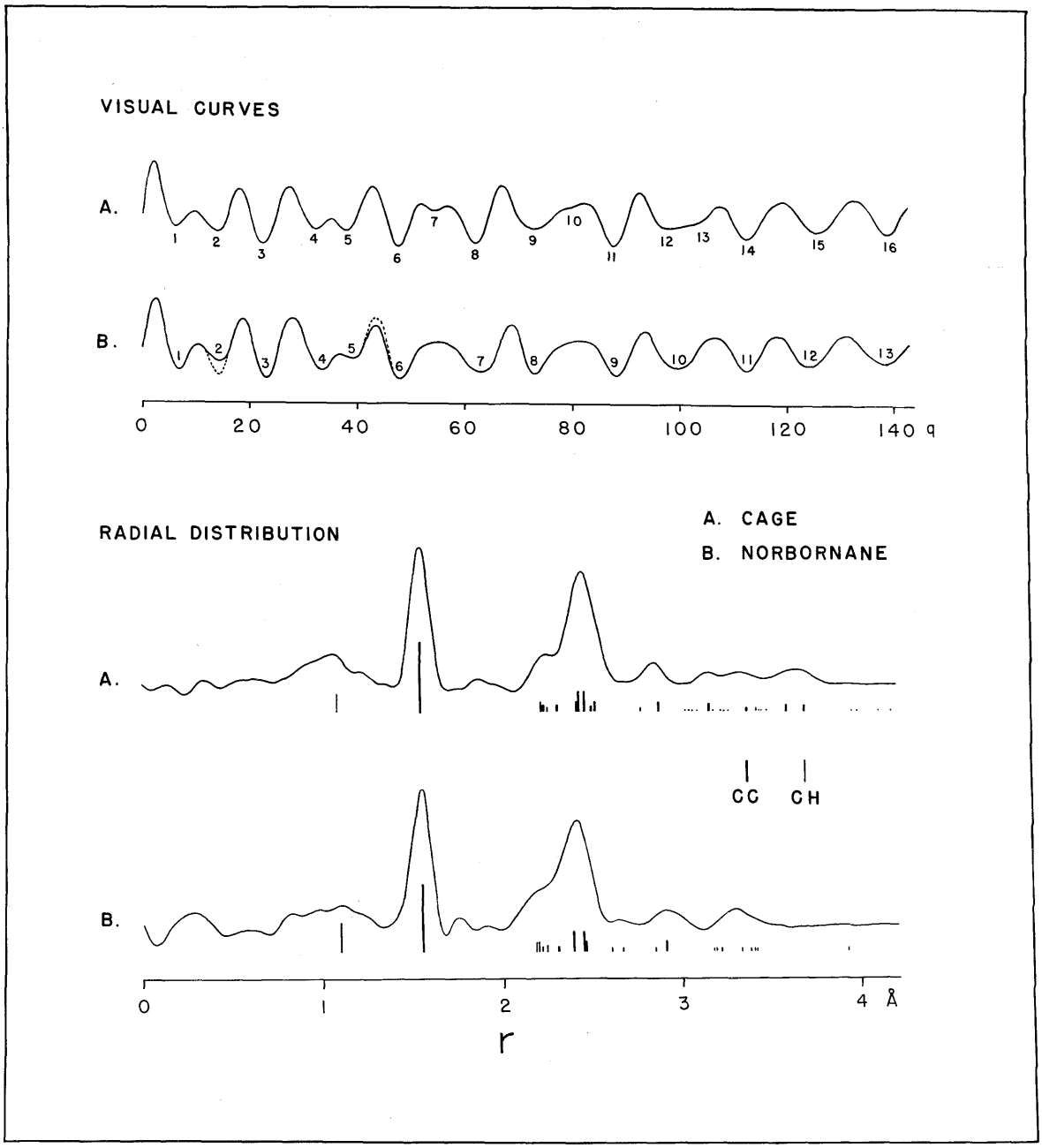
VISUAL CURVES
A.
1 2 3 4 5 6 7 8 9 10 11 12 13 14 15 16
B.
1 2 3 4 5 6 7 8 9 10 11 12 13
0 20 40 60 80 100 120 140 q
RADIAL DISTRIBUTION
A. CAGE
B. NORBORNANE
A.
CC CH
B.
0 1 2 3 4 Å
r

peaks, a sharp peak around 1.56 A and a broader peak around 2.45 A, indicative of the presence of puckered five-membered rings. The visual curves and RDI's thus confirm the structural similarity between these two compounds and indicate a lengthening of the average C-C single bond in both.

In order to make any detailed conclusion concerning the proposed cage-like model, and to obtain structural parameters of interest for both molecules, the correlation method was employed to refine the parameter values deduced from the structural formulae (fig. 1) and the RDI's.

On the assumption of C_{2v} symmetry, the carbon skeleton of the cage has nine parameters, and the norbornane skeleton five parameters. As a first approximation, all bonded C-C distances were assumed equal, leaving for the cage a four-parameter problem (one scale factor and three shape parameters), and for norbornane, a three-parameter problem (one scale factor and two shape parameters). The three shape parameters for the cage are taken as $\angle$ 242', $\angle$ 232''' (fig. 1a), and the dihedral angle γ between plane 2-3-2''' and the plane bisector of the dihedral angle formed by planes 4-4'-2'''-2 and 1-1'''-2-2''', which is taken as positive if atom 3 lies on the same side of the plane bisector as atom 4. The two shape parameters for norbornane are $\angle$ BCB' and $\angle$ABA' (fig. 1b).

In the case of the cage, the initial assumption of $\gamma = 0$ seems reasonable in view of the approximate symmetry of the molecule

about the 2-3-2''' plane. The remaining two-parameter problem was then extensively investigated.* Representative theoretical curves in the range $103^\circ \leq \angle 242' \leq 109^\circ$ and $89 \leq \angle 232''' \leq 99$ are shown by curves 1-8 in fig. 3. (The parameters used in calculating these models are tabulated in Table 1.)

For $\gamma = 0$ the range of acceptability may be interpreted as follows. Features below q = 40 are essentially invariant over the range of parameters illustrated. The observation that minimum 8 is deeper than the average of minima 6 and 9** is not represented satisfactorily by curves 6, 7, and 12.*** Curve 5 is on the borderline. The acceptability of this feature is improved in the direction of curves 1, 2 and 8. The shape of minimum 9 was observed to be round and broad and is not represented satisfactorily by curves 7, 8 and 12.*** Curve 1**** was judged to be unacceptable since maximum 12 lies inside the broad minimum

---

* In both compounds the C-H bond length was taken to be 1.09 A. Hydrogen atoms bonded to bridge-head carbon atoms were assumed to be equidistant from the three carbon atoms bonded to the bridge-head atoms, and hydrogen atoms bonded to secondary carbon atoms were symmetrically placed with $\angle$ H-C-H equal to 109° 28'. (These are very rough approximations.)

** A three-fold comparison in which the features compared do not have the same shape is subject to systematic error. However, in this case, careful direct comparisons with the corresponding features for norbornane (fig. 2) were made, so that we are rather confident of our assessment of minima 6, 8 and 9.

*** Not shown.

**** Also curves 11 and 12 which are not illustrated.

Table 1

Cage Parameters of Fig. 3

Model	∠232'''	∠242'	γ	$a_{C.C}^{1}$	$a_{C..C}^{2}$	a_{C-H}	$a_{C.H}^{1}$	$a_{C..H}^{2}$
				(10^4A^2)	(10^4A^2)	(10^4A^2)	(10^4A^2)	(10^4A^2)
1	89.8	106.5	0	0	0	∞	∞	∞
2	91.2	"	"	"	"	"	"	"
3	93.4	"	"	"	"	"	"	"
4	95.5	"	"	"	"	"	"	"
4a	"	"	"	4.5	7.0	"	"	"
4b	"	"	"	4.5	7.0	23	35	≥ 35[3]
4c	"	"	"	10.1	10.1	23	35	≥ 35[3]
4d	"	"	"	4.5	7.0	16	25	≥ 25[3]
5	96.6	"	"	0	0	∞	∞	∞
6	98.3	"	"	"	"	"	"	"
7	95.5	103.5	"	"	"	"	"	"
8	95.5	109.6	"	"	"	"	"	"
9	95.5	106.5	-5°	"	"	"	"	"
10	95.5	106.5	+5°	"	"	"	"	"
11[4]	90.4	109.6	0	"	"	"	"	"
12[4]	90.4	103.5	0	"	"	"	"	"

1 Bonded to the same atom.

2 Not bonded to the same atom.

3 For individual values, see Table 2.

4 Not illustrated in fig. 3.

Fig. 3

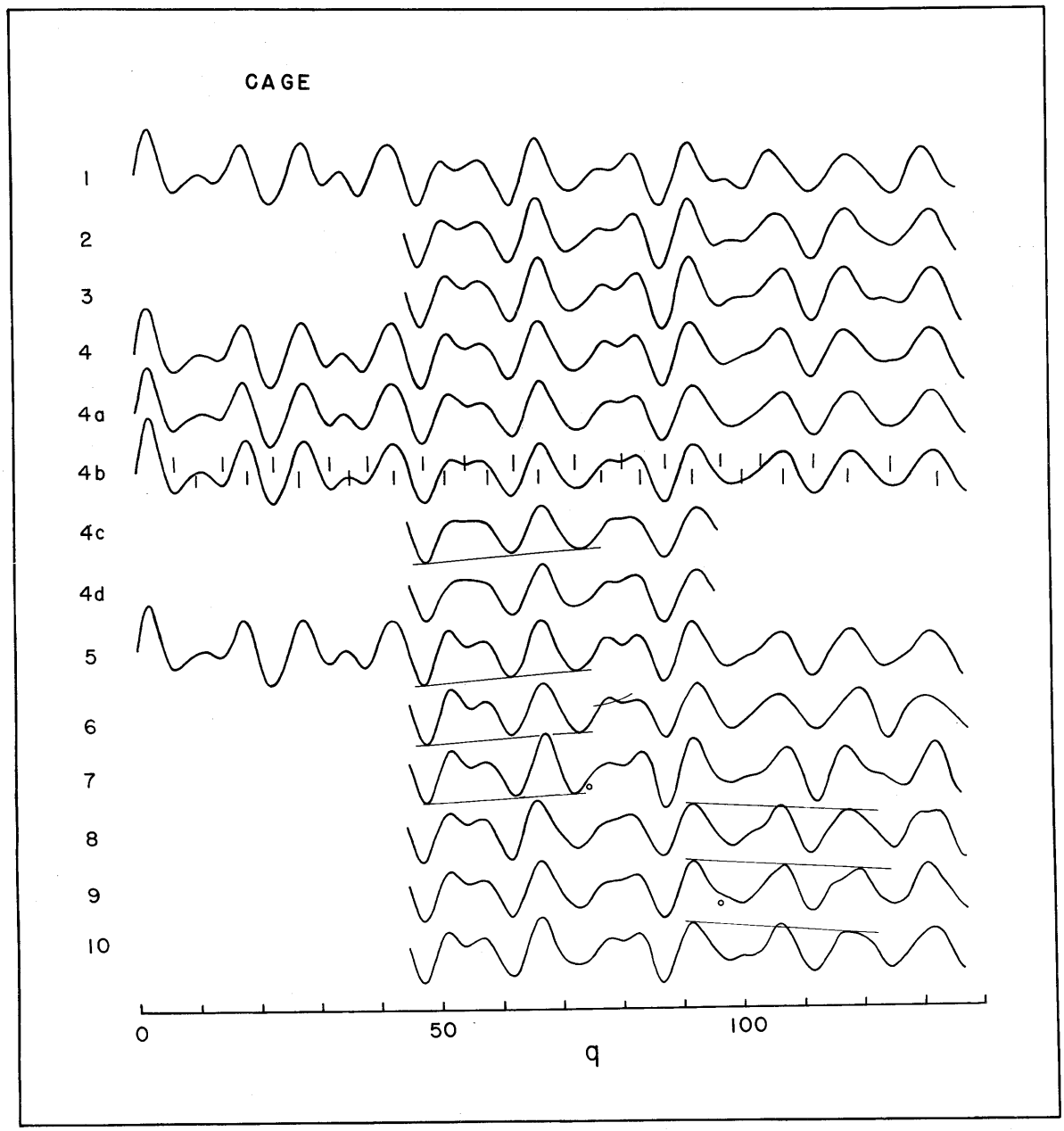

Table 2

Interatomic Distances for model 4b

	Terms	Multiplicity	Distances A	a_{ij} $10^4 A^2$
I	C-C	17	1.56	0
II	C.C			
	1-4	4	2.42	4.5
	2-4'	4	2.46	"
	1-1''	2	2.21	"
	1-2'	4	2.52	"
	1-2'''	4	2.46	"
	2-2'''	2	2.31	"
	2-2'	2	2.50	"
	3-4	4	2.43	"
	1-3	4	2.43	"
III	C..C			
	1-4'	4	2.88	7.0
	1-2''	4	3.16	"
	2-2''	2	3.40	"
	1-3'	4	3.57	"
	2-3'	4	3.69	"
	3-3'	1	4.48	"

Table 2 (Cont'd)

	Terms	Multiplicity	Distances A	a_{ij} $10^4 A^2$
IV	C-H	14	1.09	23
V	C.H			
	α' -1',1''',2	12	2.29	35
	β' -1,4,3	12	2.27	35
	γ_1', γ_2' -2	8	2.23	"
	δ_1' -1,1,4'	6	2.24	"
VI	C..H			
	δ -1	4	3.42	∞
	δ -1''	4	3.93	35
	δ -2''	4	3.27	35
	δ -3	4	2.97	"
	α -4	4	3.42	"
	α -4'	4	3.96	"
	α -1''	4	3.04	∞
	α -2'	4	3.33	"
	α -2''	4	3.41	"
	α -3	4	3.07	"
	α -3'	4	4.55	"
	β -4'	4	3.44	35
	β -1'	4	3.44	∞

Table 2 (Cont'd)

Terms	Multiplicity	Distances A	a_{ij} $10^4 A^2$
β -1''	4	4.13	35
β - 1'''	4	3.20	"
β - 2'''	4	3.06	∞
β - 2''	4	4.40	"
β - 2'	4	3.35	"
β - 3'	4	4.44	"
γ_1 -4	4	3.42	"
γ_1 -1	4	2.72	35
γ_1 - 1'	4	4.13	∞
γ_1 - 2'	4	4.54	"
γ_1 - 3'	2	5.37	"
γ_2 -1'	4	4.44	"
γ_2 - 2'	4	4.20	"
γ_2 - 3'	2	4.90	"
γ_2 -4	4	3.42	"

1 α - Hydrogen bonded to 1
β - " " to 2
γ_1 - (above plane 232''') bonded to 3
γ_2 - (below " ") " " "
δ - " " 4.

between maxima 11 and 13 and curve 2 is on the borderline. Increasing ∠232''' makes this feature acceptable. On curves 8 and 11 maximum 13 is above the average of maxima 11 and 14 which does not represent the visual observations satisfactorily. Minimum 15 is too sharp and deep on curves 1 and 6 and this feature cannot be improved, we believe, by changing the temperature factors. The general appearance of minimum 15 on curves 7 and 8 is not satisfying. The range of acceptability, assuming $\gamma = 0$, is illustrated in fig. 4. For models inside the range of acceptability, excellent agreement with the visual curve can be obtained by adjusting temperature factors and including hydrogen terms, as shown by curve 4b.

Curves 4, 9 and 10 illustrate the effect of variation of γ. The three-fold comparison among minima 6, 8 and 9 is improved by increasing γ (curve 10) while decreasing γ (curve 9) has no significant effect. A decrease of γ shifts maximum 12 to the inside of the broad minimum between maxima 11 and 13. The three-fold comparison among maxima 11, 13 and 14 becomes unsatisfactory by varying γ in either direction. Curve 9 is unacceptable while curve 10 is barely acceptable. Therefore for the values of ∠232''' and ∠242' for model 4, the indication is that $\gamma = 1^{\circ} \pm 4^{\circ}$. It is indicated that curve 5 may be made completely acceptable by slightly increasing γ since the three-fold comparison among minima 6, 8 and 9 may be made acceptable without destroying the acceptability of the comparison among maxima 11, 13 and 14.

From the above considerations we conclude that the proposed structural formula is consistent with the electron diffraction pattern. A curve was calculated (not shown) based on model 4 with the C-C bonded distances varied in a manner indicated by the bond strain calculation (see later text) without changing the average distance. No significant effect on the appearance of the curve was observed. No further attempt at differentiating the C-C bond lengths was made in view of the formidable number of parameters involved.

In the case of norbornane the range of acceptability (fig. 6) appears to be larger than for the cage. The parameters used in calculating the models are listed in Table 2, and the calculated curves are shown in fig. 5. Curves B, C, G and J are clearly unacceptable because of the shape of maximum 6 and/or 8 (G and J also failed in the three-fold comparison of minima 7, 8 and 9), while curves A, F and H are at the limit of the range of acceptability. Curve E was adjudged to represent the best model and gives excellent agreement with the visual curve. As in the case of the cage all models within the range of acceptability can be made to give good agreement with the visual curve and no effort was made to resolve the differences in the C-C bond lengths.

Calculations of the expected bond strain due to cross-ring repulsions were made for models within the range of acceptability. If a Hooke's Law potential is assumed for bond stretching and for first neighbor repulsions (the valence deformation forces are assumed negligible), then the force on atom i due to atom j can be expressed as (see Table 5):

Table 3

Norbornane Parameters of Fig. 5

Model	∠BCB'	∠ABA'	$a_{C.C}$ (10^4A^2)	a_{C-H} (10^4A^2)	$a_{C.H}$ (10^4A^2)	$a_{C..H}$ (10^4A^2)
A	98.7	104.8	4.5	16.0	41.0	80.0
B	96.3	115.3	"	"	"	"
C	96.3	108.8	"	"	"	"
D	"	105.2	"	"	"	"
E	"	"	10.1	"	"	"
F	"	101.5	4.5	"	"	"
G	"	96.0	4.5	"	"	"
H	95.0	101.7	10.1	"	"	"
I	93.0	105.8	10.1	"	"	"
J	90.5	106.5	4.5	"	"	"
K[1]	90.5	115.8	4.5	"	"	"
L[1]	98.7	113.5	"	"	"	"
M[1]	90.5	97.2	"	"	"	"
N[1]	98.7	95.5	"	"	"	"

[1] Not illustrated in Fig. 5

Fig. 5

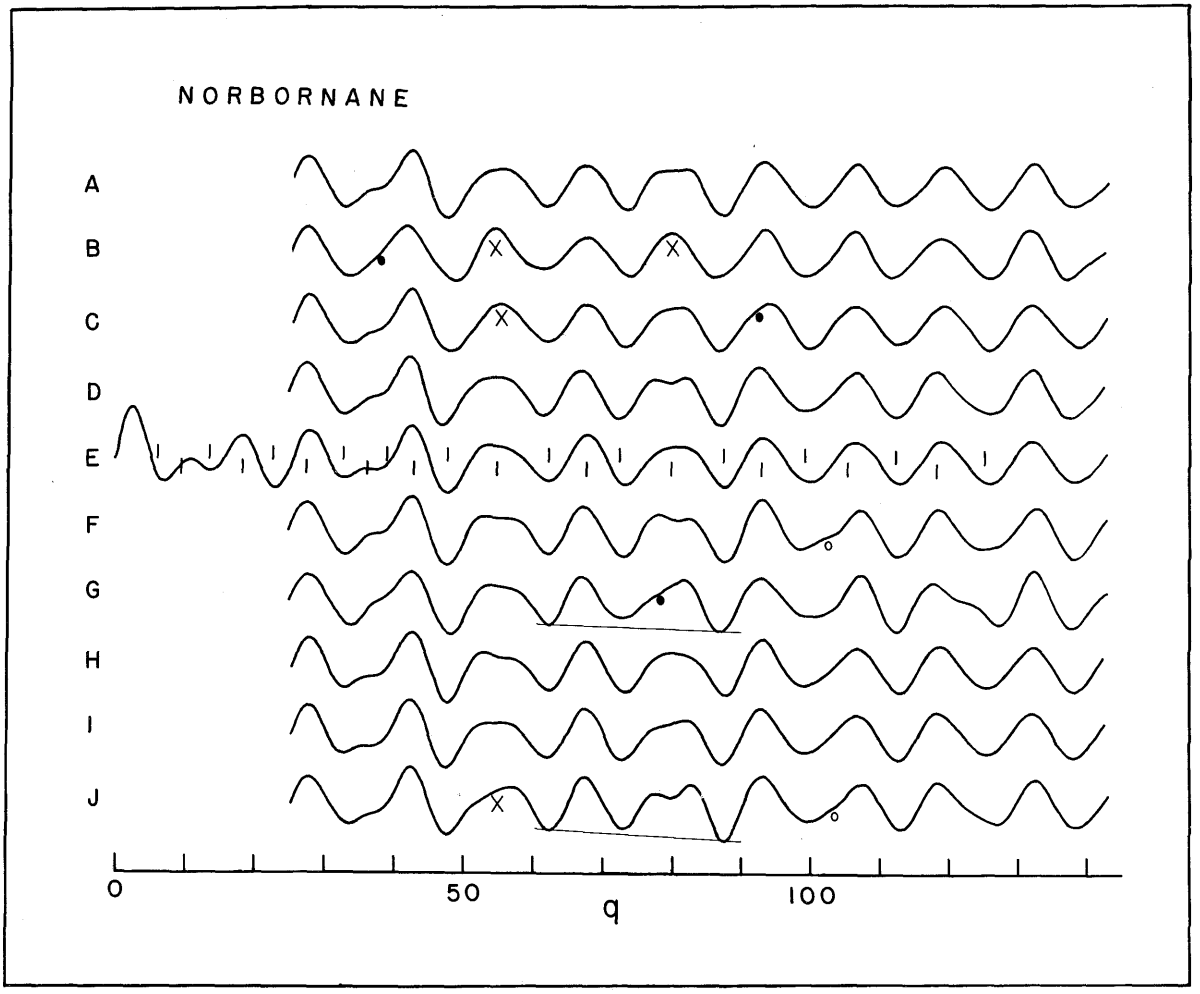

Table 4

Interatomic Distances for model E

	Terms		Multiplicity	Distances A	a_{ij} $10^4 A^2$
I	C-C		8	1.55	0
II	C...C				
		AC	4	2.39	10.1
		AB'	4	2.45	"
		BB'	1	2.31	"
		AA'	2	2.46	"
III	C...C				
		AA''	2	2.91	"
IV	C-H		12	1.10	16
V	C.H				
		β^1-B	4	2.19	41
		β-A'''	4	2.19	"
		α^1-A'''	4	2.20	"
		α-B	4	2.20	"
		δ^1-B	4	2.22	"
		γ^1-A	4	2.25	"
		γ-C	2	2.25	"
VI	C..H				
		α-A'	4	2.60	80
		δ-A	4	2.66	"
		β-C	4	2.85	"
		β-B'	4	3.18	"
		α-B'	4	3.19	"
		α-A''	4	3.22	"
		γ-B'	2	3.33	"
		α-C	4	3.36	"
		δ-A'	4	3.41	"
		γ-A'''	4	3.43	"
		β-A'	4	3.44	"
		β-A''	4	3.93	"

Table 4 (Cont'd)

---

1 α, Bonded to A (lies on the same side of plane A-A'-A''-A''' as C and B).

β, " " A.

γ, " " B.

δ, " " C.

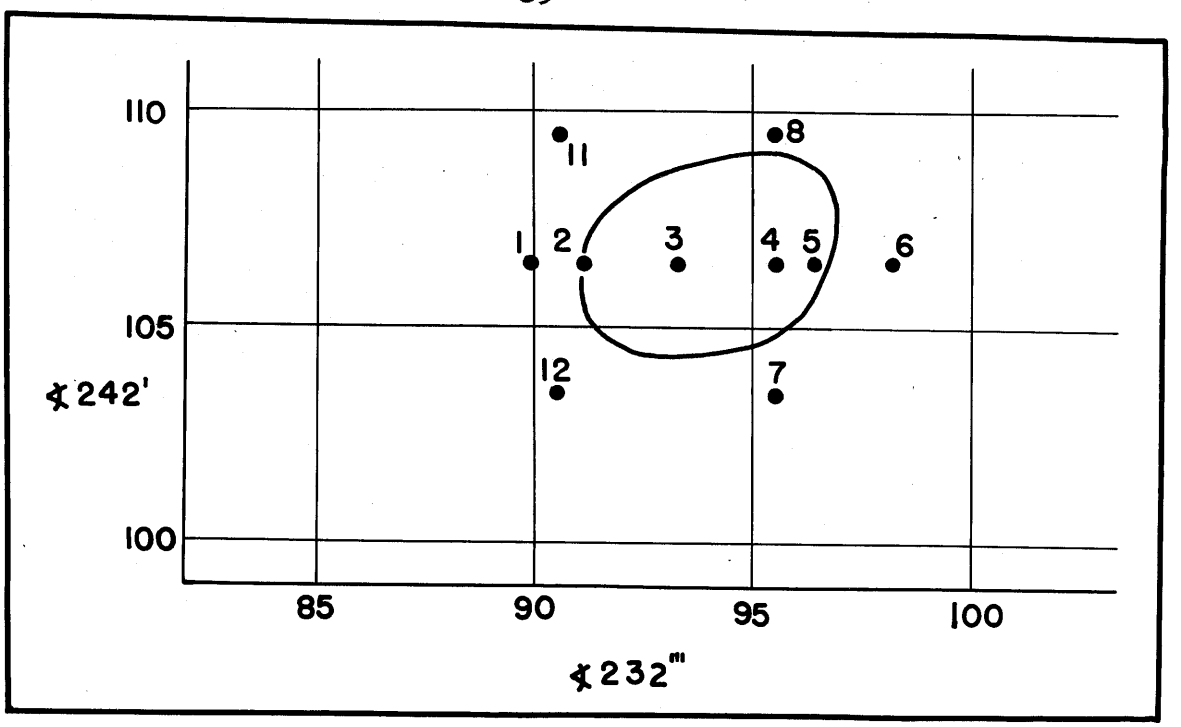
110
105
100
85
90
95
100
∢242'
∢232'''
1
2
3
4
5
6
7
8
11
12

Fig. 4

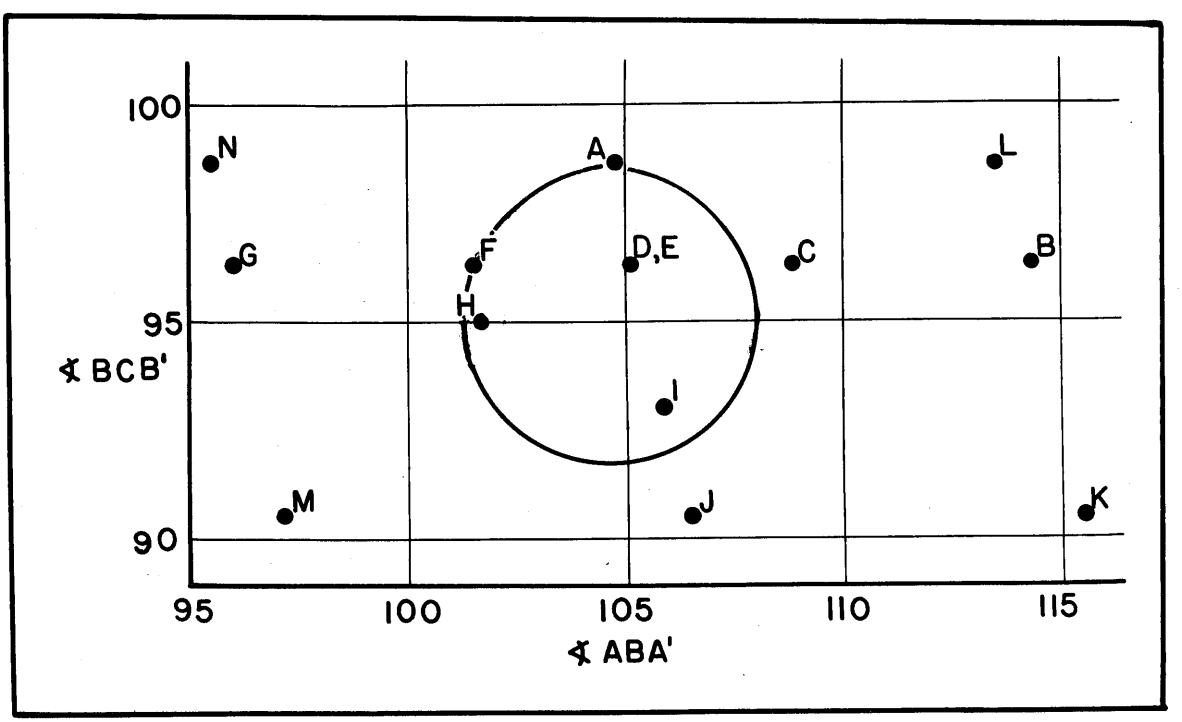
100
95
90
95
100
105
110
115
∢BCB'
∢ABA'
A
B
C
D,E
F
G
H
I
J
K
L
M
N

Fig.6

$$\underline{F}_{ij} = F_{T_{ij}} \frac{\underline{r}_j - \underline{r}_i}{r_{ij}} \qquad \text{for bond stretching,}$$

$$\underline{F}_{ij} = F_{\hat{R}_{ij}} \frac{\underline{r}_j - \underline{r}_i}{R_{ij}} \qquad \text{for repulsion}$$

where

$F_{T_{ij}}$ = tension on bond between atoms i and j

$F_{\hat{R}_{ij}}$ = repulsive force between atoms i and j,

$\underline{r}_k$ = vector from origin to atom k

$r_{ij} = |\underline{r}_i - \underline{r}_j|$, bonded; $R_{ij} = |\underline{r}_i - \underline{r}_j|$, nonbonded first neighbors.

For equilibrium $\sum_{ij} \underline{F}_{ij} = 0$ for all atoms i. In the actual calculations all vectors were resolved into Cartesian coordinates. The scheme followed was to solve the equations for the magnitudes of the repulsive and tensile forces for each model, as is possible because $\underline{r}_k$ is known from the parameters of the model, rather than to solve for the equilibrium configuration on the basis of assumed force constant values. However, there are more unknowns than equations. In order to solve these equations, the minimum number of repulsive forces (consistent with Hooke's Law, $F_{\hat{R}_{ij}} = k_1(R_{ij} - R_o)$) (Table 5) were assumed* and the

---

* For the cage the results of independent calculations by A.B. and C.W. are listed. C.W. chose the repulsive forces to be equal to $k_1(R_{ij} - R_o)$ whereas A.B. chose slightly different forces in an attempt to accomplish a rough "least square" result. For norbornane $F_{\hat{R}_{ij}} = k_1(R_{ij} - R^\circ)$ was chosen.

remaining repulsive and tensile forces calculated. The results of these calculations are listed in Table 5 for cage model 4 and norbornane model E.

The calculated values for the bond lengths in the cage and norbornane are respectively 1.560 A and 1.557 A (Table 5), in surprising agreement with the experimental values of $1.56_3 \pm 0.01$ A (Table 6) and $1.55_5 \pm 0.01$ A (Table 7).

The electron diffraction result (for $\gamma = 0$, fig. 4) indicates that model 3 is the 'best model' for the cage. However, model 4 was chosen to be the best model considering both the electron diffraction result and for consistency with the above simple calculation*. In the case of norbornane, the best electron diffraction model is consistent with the calculation.

---

* The indication is that by increasing γ, the range of acceptability of $\angle 232'''$ and $\angle 242'$ would expand in the general direction of models 4 and 5. This would presumably push model 4 (with $\gamma > 0$) toward the center of the range of acceptability in three-dimensional shape parameter space. Although the assumptions on which the bond strain calculations are based force $\gamma = 0$, the very approximate nature of these calculations cannot be ignored.

Table 5

Summary of Bond Stretching Calculations

Cage (Model 4)

F_R^1	R^o-R_{ij} (A)	Assumed Forces A.B.	Calc. Forces A.B.	Assumed Forces C.W.	Calc. Forces C.W.
1-3	.09		$.098k_1$	$.09k_1$	
1-4	.10	$.086k_1$		$.10k_1$	
1-1''	.31	$.31k_1$		$.31k_1$	
1-2'	.00	0		0	
1-2'''	.06	$.052k_1$		$.06k_1$	
2-2'	.02		$.050k_1$		$.083k_1$
2-2'''	.21		$.193k_1$		$.176k_1$
2-4'	.06	$.052k_1$		$.06k_1$	
3-4	.09	$.098k_1$			$.09k_1$

F_T^1	Calc. Tension A.B.	Calc. Stretch A.B. (A)	Calc. Tension C.W.	Calc. Stretch C.W. (A)
1-1'	$.238k_1$	.018	$.250k_1$	.019
1-1'''	$.340k_1$	.025	$.347k_1$	.026
1-2	$.199k_1$	.015	$.213k_1$	.016
2-3	$.235k_1$	.018	$.216k_1$	.016
2-4	$.219k_1$	.016	$.247k_1$	.019
4-4'	$.258k_1$	.019	$.280k_1$	.021
		Ave. Stretch .019 A		.020 A
		Stretch + 1.54 = 1.559 A ,		1.560 A

Table 5 (Cont'd)

Norbornane (Model E)

F_R	R^o-R_{ij}	Assumed Forces	Calc. Forces
A-C	.13	$.13k_1$	
B-B'	.21		$.232k_1$
A-A'	.06		$.080k_1$
A-B'	.07	$.07k_1$	

F_T	Calc. Tensions	Calc. Stretch (A)
A-B	$.229k_1$	.017
B-C	$.309k_1$	.023
A-A'''	$.153k_1$	.011

Ave. Stretch .017 A

Stretch + 1.54 = 1.557 A

1 $F_{T_{ij}} = k_2 (r_{ij} - r_o)$

$F_{R_{ij}} = k_1 (R_{ij} - R_o)$

r_o = normal C-C single-bond length

R_o = normal non-bonded distance assuming tetrahedral angle, 2.52 A

k_2 = force constant for C-C single-bond stretching, $4 \frac{md}{A}$ (6)

k_1 = force constant for C.C repulsion, $0.3 \frac{md}{A}$. (This value is assumed from the bending force constant of ∠C-C-C.) (6)

Table 6

Max.	Min.	q_o[1]	Wt.	q_c/q_o (4b)
	1	6.07		
1		9.86		
	2	14.19		
2		18.33		
	3	22.56		1.004
3		26.72		1.040
	4	31.82		1.014
4		35.14		1.002
	5	38.19		.985
5		42.60	1	.998
	6	47.33	1	1.010
6		50.95		1.022
	7	54.28		1.003
7		58.04		.977
	8	62.40	1	.996
8		66.46	1	1.005
	9	72.47		1.007
9		76.75		
	10	80.17		.998
10		83.22		
	11	87.35	1	1.000
11		91.85	1	1.004
	12	96.49		1.021
12		99.98		
	13	103.07		
13		106.83		1.001
	14	111.93	1	1.002
14		(117.65)		1.004
	15	(124.82)		
15		(132.65)		
		Ave. 7		1.002
		Ave. 22		1.005
		Mean dev. 7		.0035
		" " 22		.0088

For "cage" C-C = $1.56 \times \frac{q_c}{q_o}$ (4b) = 1.56 (1.002) = 1.563

[1] Ave. of C.W., A.B. and V.S.
( ) V.S. only

Table 7

Max.	Min.	q_o^1	q_c/q_o (E)	Wt.
	1	6.07		
1		9.46		
	2	13.55		
2		18.38		
	3	22.64	1.014	
3		27.48	1.021	
	4	32.75	1.011	
4		36.12		
	5	38.96		
5		42.92	.996	1
	6	47.77	1.002	1
6		54.91		
	7	62.35	1.002	1
7		67.72	1.004	1
	8	72.47	1.012	1
8		80.07		
	9	87.54	1.002	1
9		92.99	1.003	1
	10	99.21	1.008	
10		105.34	1.011	
	11	112.58	1.004	
11		118.32	1.006	
	12	125.12		
12		128.14		
	Ave. 7		1.003	Ave. dev. .004
	Ave. 14		1.007	Ave. dev. .005

$r_{C-C} = 1.55 \times 1.003 = 1.555$

[1] Ave. of C.W., A.B. and V.S.

Table 8

The Bond Angles of Cage (4b) and the Corresponding Bond Angles of Norbornane (E)

Cage			Norbornane	
232'''	95°30'	———	BCB'	96°19
423	102°18'	———	ABC	99°43'
321	102°18			
124	101°43'	———	ABA'	105°14'
211'''	104°4'	———	BAA'''	104°11'
244'	104°4'			
242'	106°29'			
211'	107°43'			
1'11'''	90°			

References

1. L. De Vries, Ph.D. Thesis, UCLA, (1955).

2. J. D. McCullough, Private communication.

3. J. D. Dunitz and V. Schomaker, J. Chem. Phys. 20, 1703-7 (1952).

4. E. Heilbronner and V. Schomaker, Helv. Chim. Acta, 173, 1385-1404, (1952).

5. K. Hedberg and J. A. Stosick, J. Am. Chem. Soc., 74, 954-8 (1952).

6. D. M. Gates, J. Chem. Phys., 17, 393-8 (1949).

Ph.D. Final Examination--------Chi-hsiang Wong

Committee: Professor Schomaker (Chairman),
Drs. Bergman, Buchman, Marsh and Cowan

Wednesday, May 15, 1957----1:30 P.M., Crellin Conference Room

Thesis Title: The Study of a Crystal Structure by X-ray Diffraction and Some Molecular Structures by Electron Diffraction.

PROPOSITIONS

1. In order to check the differences in C-C bond lengths in the polycyclohydrocarbons predicted from our simple assumption on bond stretching and cross-ring repulsion effect, a precise crystal structure determination of one of the strained polycyclohydrocarbons seems quite necessary. A method to prevent the spinning of the polycyclohydrocarbon molecule in the crystal is suggested.

2. The presence of valence electrons may be detected by a careful X-ray diffraction study of such a series of gaseous compounds as ethane, ethylene and acetylene.

3. The structure of CI_3H has been determined by X-ray diffraction of the single crystal (C-I = 2.18 ± 0.06 A, ∠I-C-I = 109 ± 5°) (1) and by electron diffraction of vapor (C-I = 2.12 ± 0.04 A , ∠I-C-I = 113°) (2). A reinvestigation is in order since neither determination can be considered as reliable. The error in the X-ray work is explained.

4. The electron exchange reaction

$$Mn^{*}O_4^{-} + MnO_4^{=} \rightarrow MnO_4^{-} + Mn^{*}O_4^{=}$$

has been investigated (3); no definite conclusion was drawn on the mechanism of the exchange (electron transfer through the solvent or atomic exchange). A method is proposed to identify the mechanism.

5. Calculated X-ray form factors for heavy atoms are usually based on the Thomas-Fermi model. This approximation seems to be not very good and leads to anomalous temperature factor corrections. Careful low-temperature experimental determinations of form factors for heavy atoms are needed.

6. The following structures have been proposed for the new antibiotic oxamycin based on degradation reaction and infrared study (4) (5).

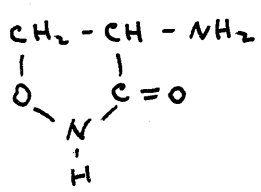

(1)

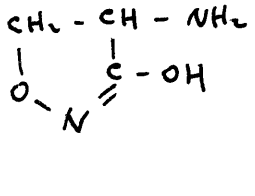

(2)

A NMR proton spectrum would certainly be able to single out the right structure.

7. The niobium-sulfuric acid complex is colorless for Nb^{+5}, and red for Nb^{+3}. However, the red complex in contact with air turns into blue color in a short time and then colorless. A paramagnetic resonance study may give some evidence of whether the blue color is due to the presence of a Nb^{+4} complex.

8. The observed strain energy in cyclopropane and cyclobutane is in agreement with the value estimated from the compression of the C-C-C bond angle with varied force constant. The force constants are determined from the spectroscopic data.

9. As a long standing foreign student (7.5 years), I believe that exchange students and scholars on a large scale between two not very friendly nations is an effective means to release the international tension. Caltech as a leading Institute in this country should start such a program immediately.

REFERENCES

(1) A. I. Kitaigorodskii, T. L. Khosyanova and Yu. T. Strushkov, Zhur. Fiz. Khim. 27, 647-56 (1953).

(2) O. Bastiansen, Tid skr. Kemi Bergv. Met. 6, 1 (1946).

(3) J. C. Sheppard and A. C. Wahl, J. Am. Chem. Soc. 75, 4188-9 (1953).

(4) F. A. Kuel, Jr., F. J. Wolf and others, J. Am. Chem. Soc. 77, 2344-5 (1955)

(5) D. A. Harris, M. Ruger and others, J. Am. Chem. Soc. 77, 2345-6 (1955).